Solid electrolytes for battery applications – a theoretical perspective*

N. A. W. Holzwarth**

Department of Physics

Wake Forest University, Winston-Salem, NC, USA, 27109

- Motivation and background information
- Overview of computational methods
- Some representative results

*Supported by NSF Grants DMR-0705239 and DMR-1105485 and WFU's Center for Energy, Environment, and Sustainability.

**With help from Nicholas Lepley (physics graduate student), Yaojun Du (previous physics postdoc) and colleagues from WFU chemistry department – Dr. Keerthi Senevirathne, Dr. Cynthia Day, Professor Michael Gross (visiting from Bucknell U.) and Professor Abdessadek Lachgar.

Materials components of a Li ion battery

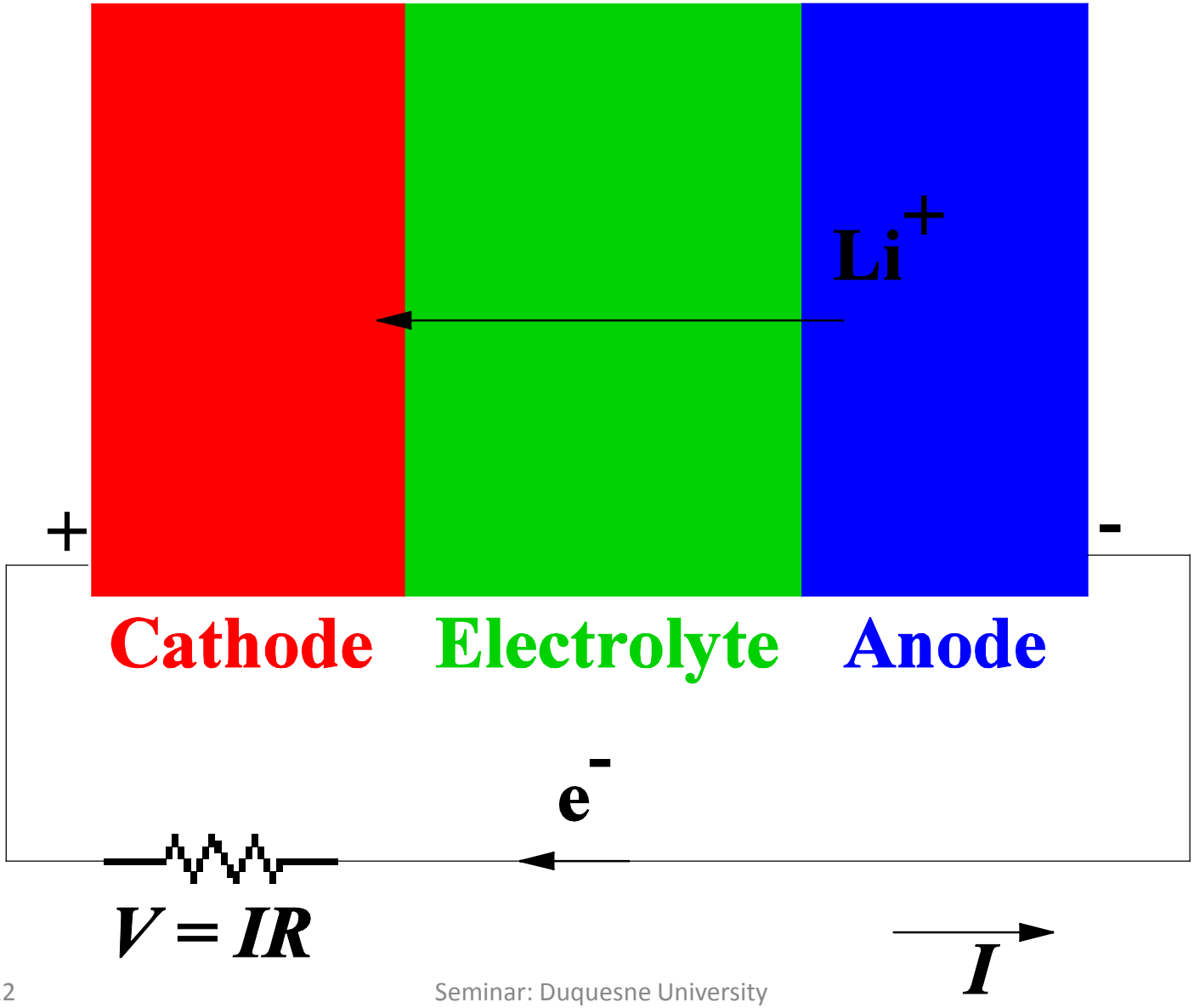

Example: Thin-film battery developed by Nancy Dudney and collaborators at Oak Ridge National Laboratory – **LiPON** (lithium phosphorus oxinitride)

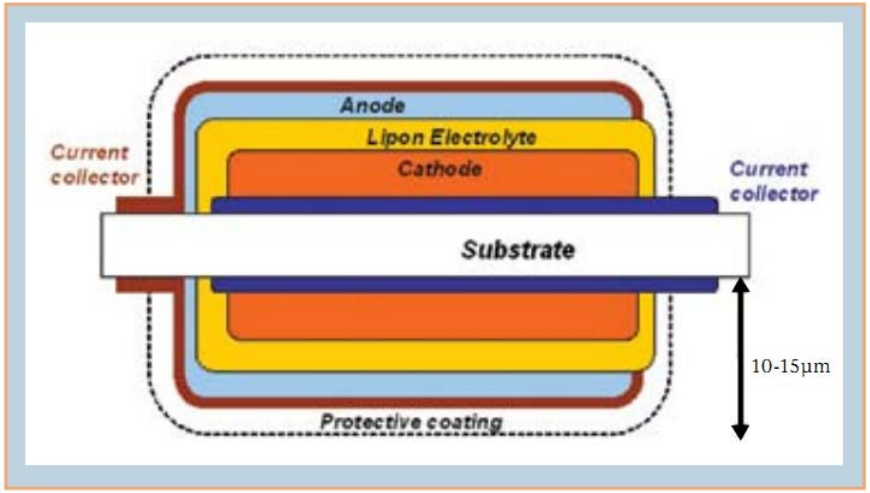

Fig. 1. *Schematic cross section of a thin film battery fabricated by vapor deposition onto both sides of a substrate support.*

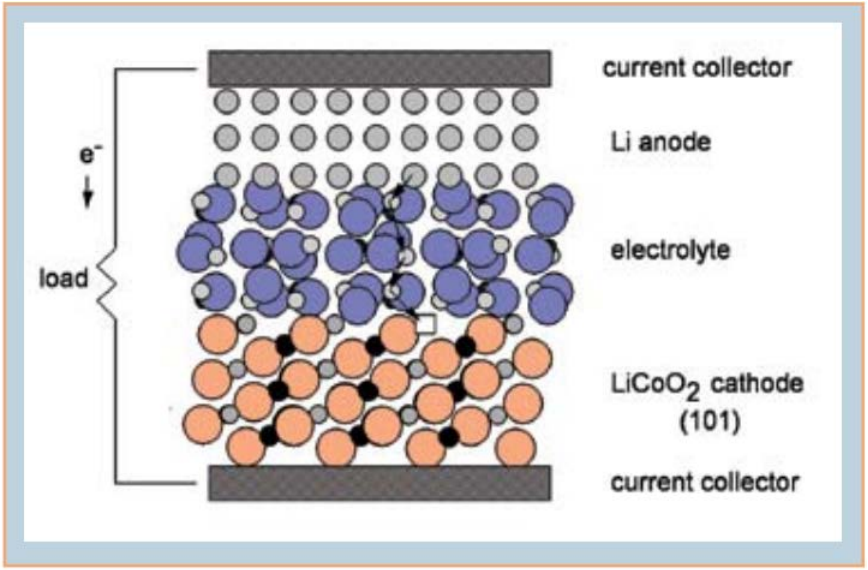

Fig. 2. *Schematic illustration of a thin film battery. The arrows indicate the discharge reaction where a Li ion diffuses from the lithium metal anode to fill a vacancy in an intercalation compound that serves as the cathode. The compensating electron is conducted through the device.*

From: N. J. Dudney, ***Interface* 77**(3) 44 (2008)

Solid *vs* liquid electrolytes in Li ion batteries

Solid electrolytes

Advantages

1. Excellent chemical and physical stability.
2. Perform well as thin film (≈1μ)
3. Li^+ conduction only (excludes electrons).

Disadvantages

1. Reduced contact area for high capacity electrodes.
2. Interface stress due to electrode charging and discharging.
3. Relatively low ionic conductivity.

Liquid electrolytes

Advantages

1. Excellent contact area with high capacity electrodes.
2. Can accommodate size changes of electrodes during charge and discharge cycles.
3. Relatively high ionic conductivity.

Disadvantages

1. Relatively poor physical and chemical stability.
2. Relies on the formation of "solid electrolyte interface" (SEI) layer.
3. May have both Li^+ and electron conduction.

Motivation: Paper by N. Kayama, *et. al* in ***Nature Materials*** **10**, 682-686 (2011)

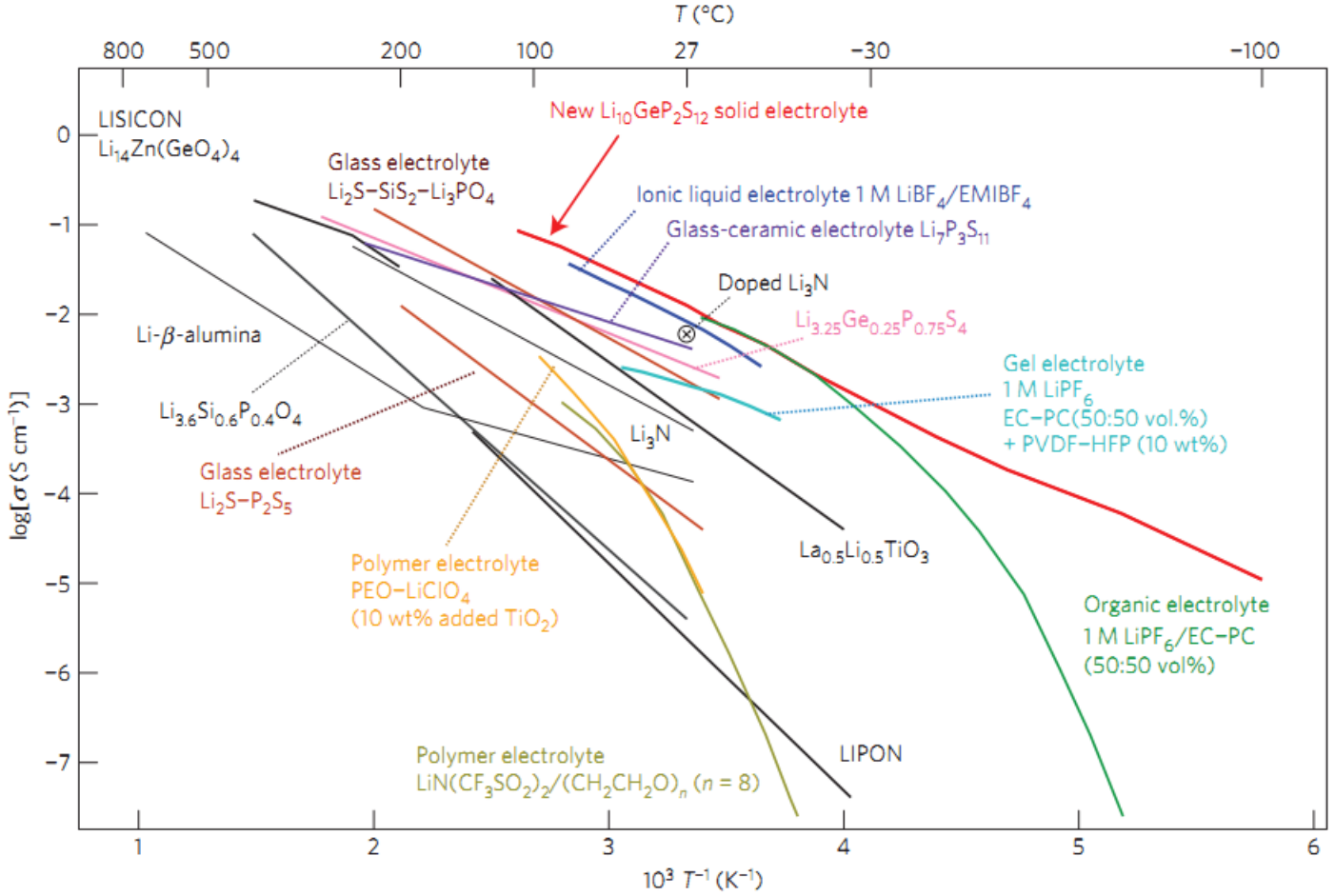

Figure 3 | Thermal evolution of ionic conductivity of the new $Li_{10}GeP_2S_{12}$ phase, together with those of other lithium solid electrolytes, organic liquid electrolytes, polymer electrolytes, ionic liquids and gel electrolytes[3-8,13-16,20,22]**.** The new $Li_{10}GeP_2S_{12}$ exhibits the highest lithium ionic conductivity (12 m S cm^{-1} at 27 °C) of the solid lithium conducting membranes of inorganic, polymer or composite systems. Because organic electrolytes usually have transport numbers below 0.5, inorganic lithium electrolytes have extremely high conductivities.

Motivation: Paper by N. Kamaya, *et. al* in ***Nature Materials*** **10**, 682-686 (2011)

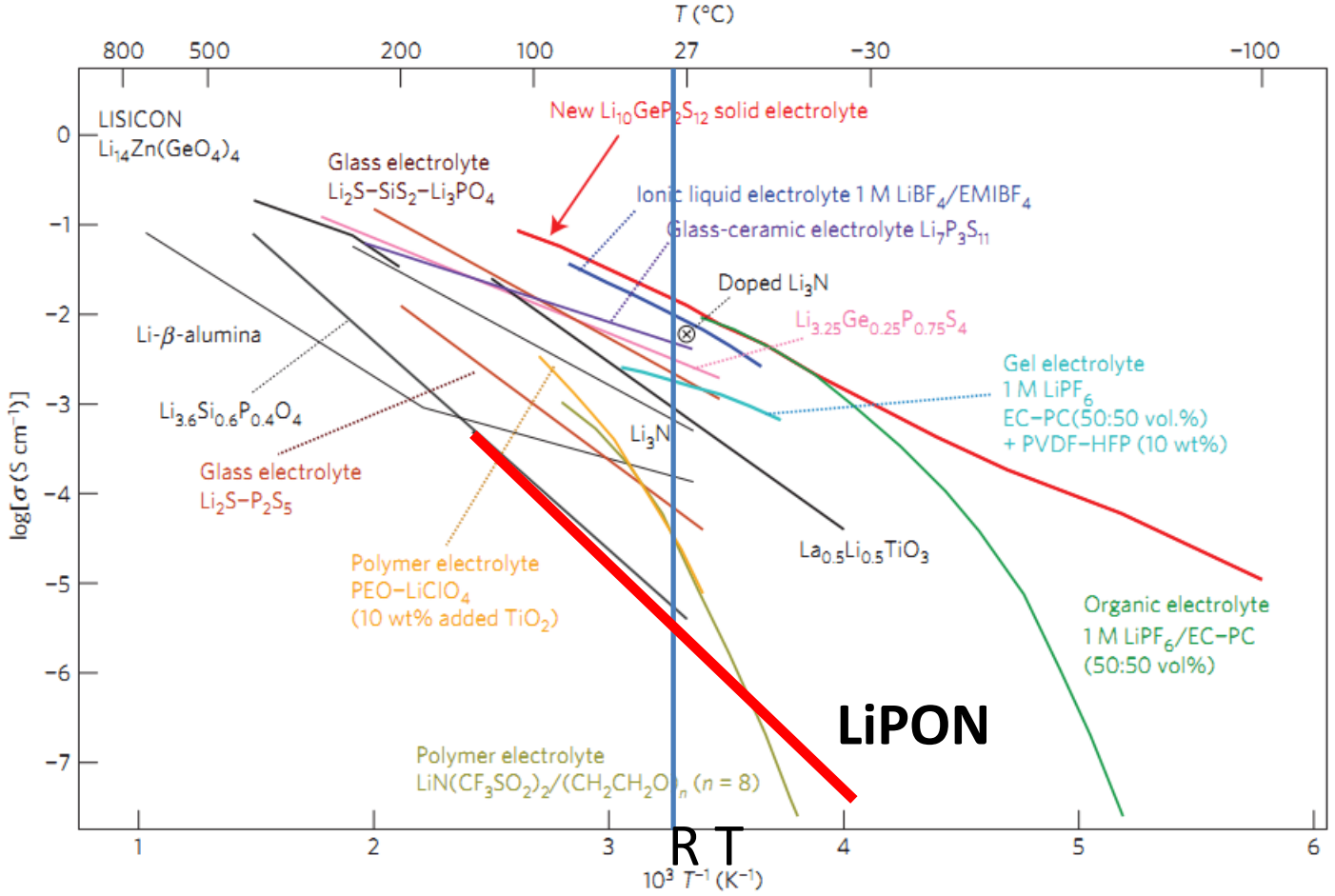

Figure 3 | Thermal evolution of ionic conductivity of the new $Li_{10}GeP_2S_{12}$ phase, together with those of other lithium solid electrolytes, organic liquid electrolytes, polymer electrolytes, ionic liquids and gel electrolytes[3-8,13-16,20,22]**.** The new $Li_{10}GeP_2S_{12}$ exhibits the highest lithium ionic conductivity (12 m S cm^{-1} at 27 °C) of the solid lithium conducting membranes of inorganic, polymer or composite systems. Because organic electrolytes usually have transport numbers below 0.5, inorganic lithium electrolytes have extremely high conductivities.

Motivation: Paper by N. Kamaya, *et. al* in ***Nature Materials*** **10**, 682-686 (2011)

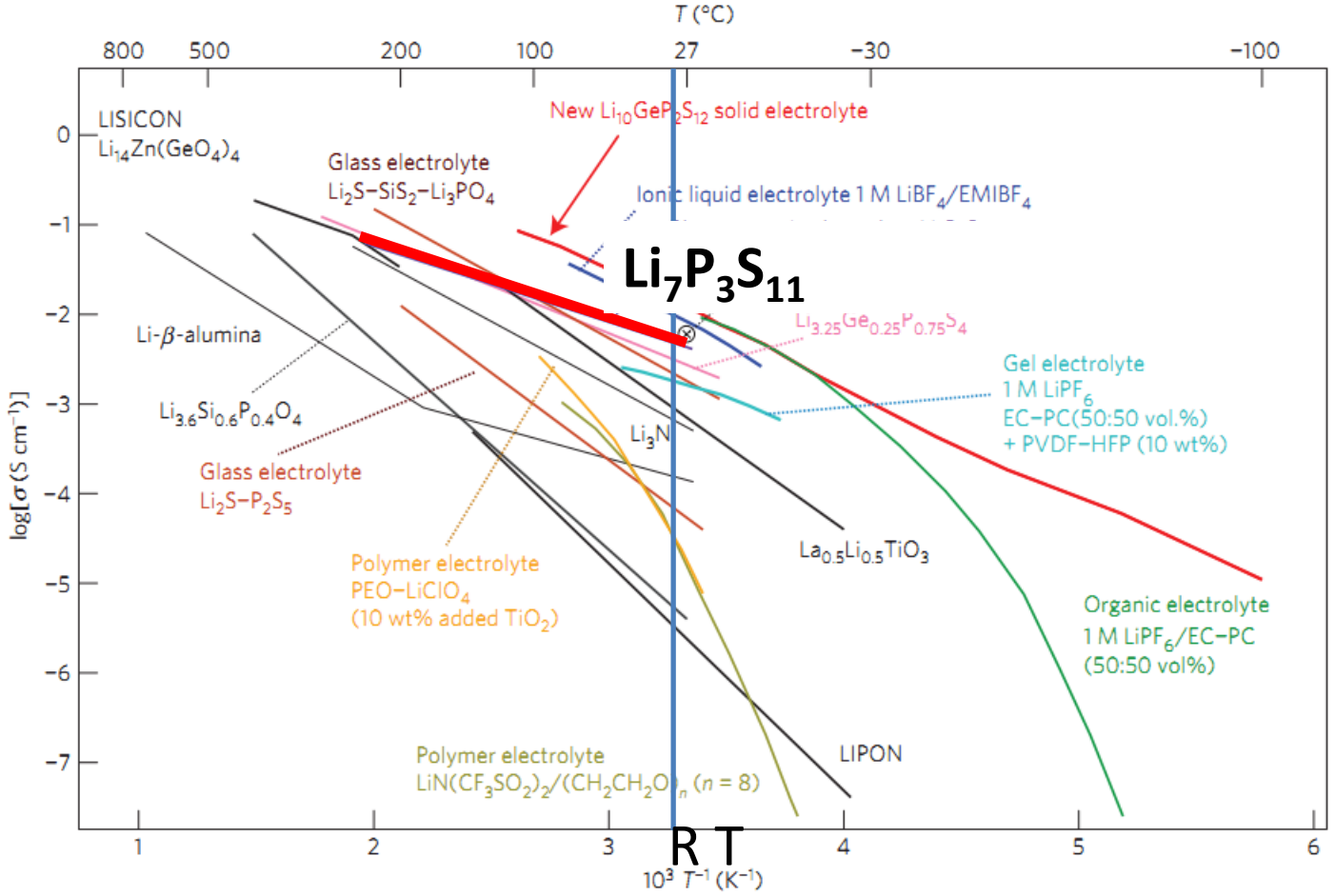

Figure 3 | Thermal evolution of ionic conductivity of the new $Li_{10}GeP_2S_{12}$ phase, together with those of other lithium solid electrolytes, organic liquid electrolytes, polymer electrolytes, ionic liquids and gel electrolytes[3-8,13-16,20,22]**.** The new $Li_{10}GeP_2S_{12}$ exhibits the highest lithium ionic conductivity (12 m S cm^{-1} at 27 °C) of the solid lithium conducting membranes of inorganic, polymer or composite systems. Because organic electrolytes usually have transport numbers below 0.5, inorganic lithium electrolytes have extremely high conductivities.

Motivation: Paper by N. Kamaya, *et. al* in ***Nature Materials*** **10**, 682-686 (2011)

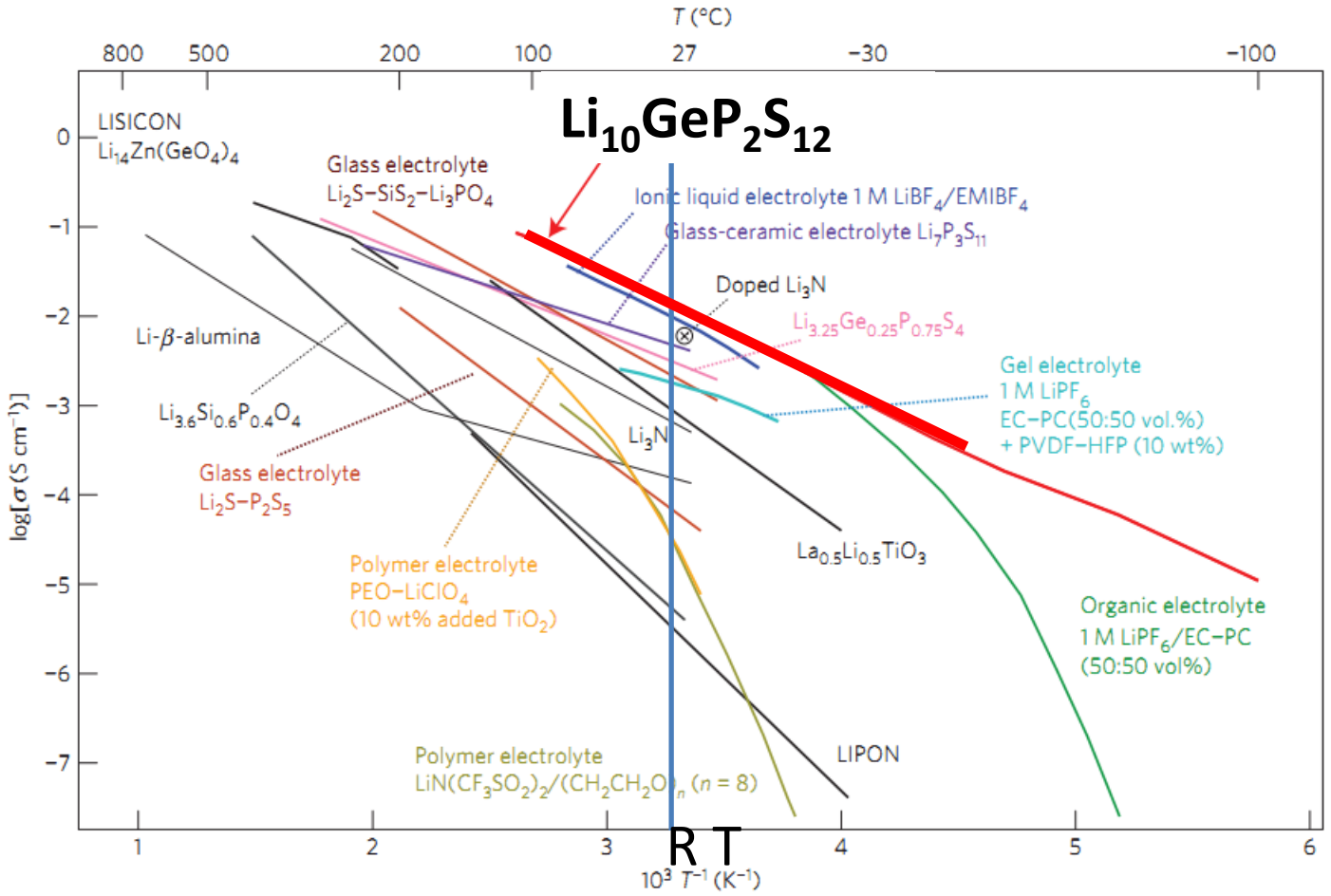

Figure 3 | Thermal evolution of ionic conductivity of the new $Li_{10}GeP_2S_{12}$ phase, together with those of other lithium solid electrolytes, organic liquid electrolytes, polymer electrolytes, ionic liquids and gel electrolytes[3-8,13-16,20,22]**.** The new $Li_{10}GeP_2S_{12}$ exhibits the highest lithium ionic conductivity (12 m S cm^{-1} at 27 °C) of the solid lithium conducting membranes of inorganic, polymer or composite systems. Because organic electrolytes usually have transport numbers below 0.5, inorganic lithium electrolytes have extremely high conductivities.

WAKE FOREST UNIVERSITY

How can computer simulations contribute to the development of materials?

- Examine known materials and predict new materials
  - Structural forms
  - Relative stabilities
  - Analyze vibrational modes and other experimentally accessible properties
- Model ion migration mechanisms
  - Vacancy migration
  - Interstitial migration
  - Vacancy-interstitial formation energies

Summary of "first-principles" calculation methods

Exact problem :

Electronic coordinates

Atomic coordinates

$$\mathcal{H}(\{\mathbf{r}_i\},\{\mathbf{R}^a\})\Psi_\alpha(\{\mathbf{r}_i\},\{\mathbf{R}^a\}) = E_\alpha \Psi_\alpha(\{\mathbf{r}_i\},\{\mathbf{R}^a\})$$

Born-Oppenheimer approximation

Born & Huang, **Dynamical Theory of Crystal Lattices**, Oxford (1954)

Density functional theory

Hohenberg and Kohn, *Phys. Rev*. **136** B864 (1964)

Kohn and Sham, *Phys. Rev*. **140** A1133 (1965)

Approximately equivalent problem :

Ground state energy (mean field approximation) : $E_0(\mathbf{r},\rho(\mathbf{r}),\{\mathbf{R}^a\})$

$$H_{eff}(\mathbf{r},\rho(\mathbf{r}),\{\mathbf{R}^a\})\psi_n(\mathbf{r}) = \varepsilon_n \psi_n(\mathbf{r})$$

$$\rho(\mathbf{r}) = \sum_n |\psi_n(\mathbf{r})|^2 \qquad H_{eff}(\mathbf{r},\rho(\mathbf{r}),\{\mathbf{R}^a\}) = \frac{\delta E_0(\mathbf{r},\rho(\mathbf{r}),\{\mathbf{R}^a\})}{\delta\rho(\mathbf{r})}$$

More computational details:

$$H_{eff}(\mathbf{r},\rho(\mathbf{r}),\{\mathbf{R}^a\}) = -\frac{\hbar^2\nabla^2}{2m} + \sum_a \underbrace{\frac{-Z^a e^2}{|\mathbf{r}-\mathbf{R}^a|}}_{\text{electron-nucleus}} + \underbrace{e^2\int d^3r' \frac{\rho(\mathbf{r}')}{|\mathbf{r}-\mathbf{r}'|}}_{\text{electron-electron}} + \underbrace{V_{xc}(\rho(\mathbf{r}))}_{\text{exchange-correlation}}$$

Exchange-correlation functionals:

- LDA: J. Perdew and Y. Wang, Phys. Rev. B **45**, 13244 (1992)
- GGA: J. Perdew, K. Burke, and M. Ernzerhof, PRL **77**, 3865 (1996)
- HSE06: J. Heyd, G. E. Scuseria, and M. Ernzerhof, JCP **118**, 8207 (2003)

Numerical methods:

- "Muffin-tin" construction: Augmented Plane Wave developed by Slater → "linearized" version by Andersen:
  - J. C. Slater, Phys. Rev. **51** 846 (1937)
  - O. K. Andersen, Phys. Rev. B **12** 3060 (1975) (LAPW)
- Pseudopotential methods:
  - J. C. Phillips and L. Kleinman, Phys. Rev. **116** 287 (1959) -- original idea
  - P. Blöchl, Phys. Rev. B. 50 17953 (1994) – Projector Augmented Wave (PAW) method

Outputs of calculations:

Ground state energy :

$E_0(\mathbf{r}, \rho(\mathbf{r}), \{\mathbf{R}^a\})$ $\Rightarrow$ Determine formation energies

$\min|_{\{\mathbf{R}^a\}}\left(E_0(\mathbf{r}, \rho(\mathbf{r}), \{\mathbf{R}^a\})\right)$ $\Rightarrow$ Determine structural parameters

$\Rightarrow$ Stable and meta - stable structures

$\Rightarrow$ Normal modes of vibration

$\rho(\mathbf{r}) = \sum_n |\psi_n(\mathbf{r})|^2$ $\Rightarrow$ Self - consistent electron density

$\{\varepsilon_n\}$ $\Rightarrow$ One - electron energies; densities of states

Estimate of ionic conductivity assuming activated hopping

Schematic diagram of minimal energy path

Approximated using NEB algorithm[a]
– "Nudged Elastic Band"

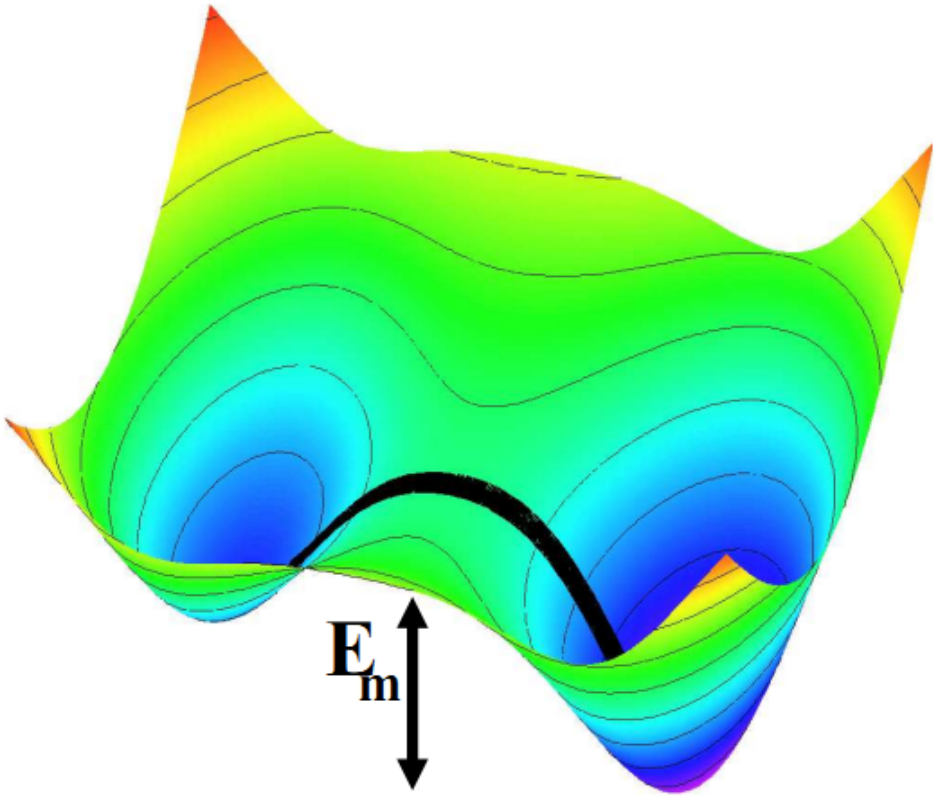

[a]Henkelman and Jónsson, *JCP* **113**, 9978 (2000)

Arrhenius relation

$$\sigma \cdot T = K e^{-E_A/kT}$$

From: Ivanov-Shitz and co-workers, *Cryst. Reports* **46**, 864 (2001):

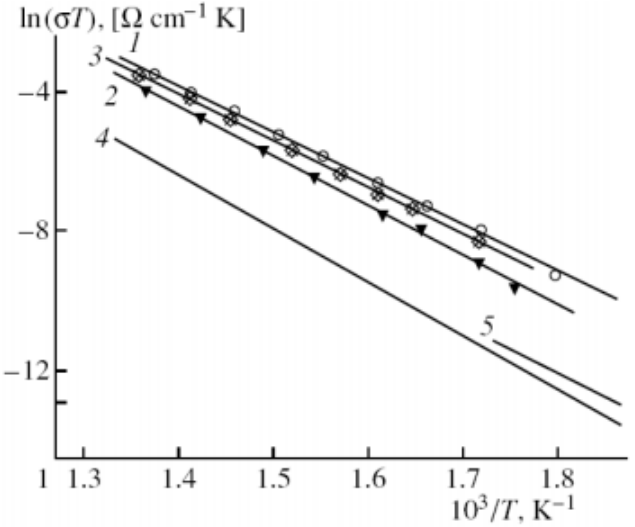

Fig. 2. Temperature dependences of conductivity in γ-Li_3PO_4: (*1*–*3*) for single crystals measured along the (*1*) *a*-axis, (*2*) *b*-axis, (*3*) *c*-axis and (*4*, *5*) for a polycrystal (*4*) according to [4, 5] and (*5*) according to [7].

E_A = 1.14, 1.23, 1.14, 1.31, 1.24 eV for 1,2,3,4,5, respectively.

Public domain codes available for electronic structure calculations

Method	Codes	Comments
LAPW	www.wien2k.at elk.sourceforge.net	Works well for smaller unit cells; variable unit cell optimization not implemented. Need to choose non-overlapping muffin tin radii and avoid "ghost" solutions.
PAW	www.abinit.org www.quantum-espresso.org	Works well for large unit cells (<200 atoms or so); includes variable unit cell optimization. Need to construct and test PAW datasets

Other efforts:

- Gerbrand Ceder's group at MIT – Materials Project; A Materials Genome Approach -- http://www.materialsproject.org/
- Stefano Curtarolo's group at Duke – Energy Materials Laboratory -- http://materials.duke.edu/

ATOMPAW Code for generating atomic datasets for PAW calculations

Holzwarth, Tackett, and Matthews, CPC 135 329 (2001) http://pwpaw.wfu.edu

Periodic Table of the Elements for PAW Functions

1 H																	2 He
3 Li	4 Be											5 B	6 C	7 N	8 O	9 F	10 Ne
11 Na	12 Mg											13 Al	14 Si	15 P	16 S	17 Cl	18 Ar
19 K	20 Ca	21 Sc	22 Ti	23 V	24 Cr	25 Mn	26 Fe	27 Co	28 Ni	29 Cu	30 Zn	31 Ga	32 Ge	33 As	34 Se	35 Br	36 Kr
37 Rb	38 Sr	39 Y	40 Zr	41 Nb	42 Mo	43 Tc	44 Ru	45 Rh	46 Pd	47 Ag	48 Cd	49 In	50 Sn	51 Sb	52 Te	53 I	54 Xe
55 Cs	56 Ba		72 Hf	73 Ta	74 W	75 Re	76 Os	77 Ir	78 Pt	79 Au	80 Hg	81 Tl	82 Pb	83 Bi	84 Po	85 At	86 Rn
87 Fr	88 Ra		104 Rf	105 Db	106 Sg	107 Bh	108 Hs	109 Mt	110 Uun	111 Uuu	112 Uub		114 Uuq		116 Uuh		
		57 La	58 Ce	59 Pr	60 Nd	61 Pm	62 Sm	63 Eu	64 Gd	65 Tb	66 Dy	67 Ho	68 Er	69 Tm	70 Yb	71 Lu	
		89 Ac	90 Th	91 Pa	92 U	93 Np	94 Pu	95 Am	96 Cm	97 Bk	98 Cf	99 Es	100 Fm	101 Md	102 No	103 Lr	

Datasets can interface with *abinit*, *quantum-espresso*, and other codes.

Test results for simple oxides

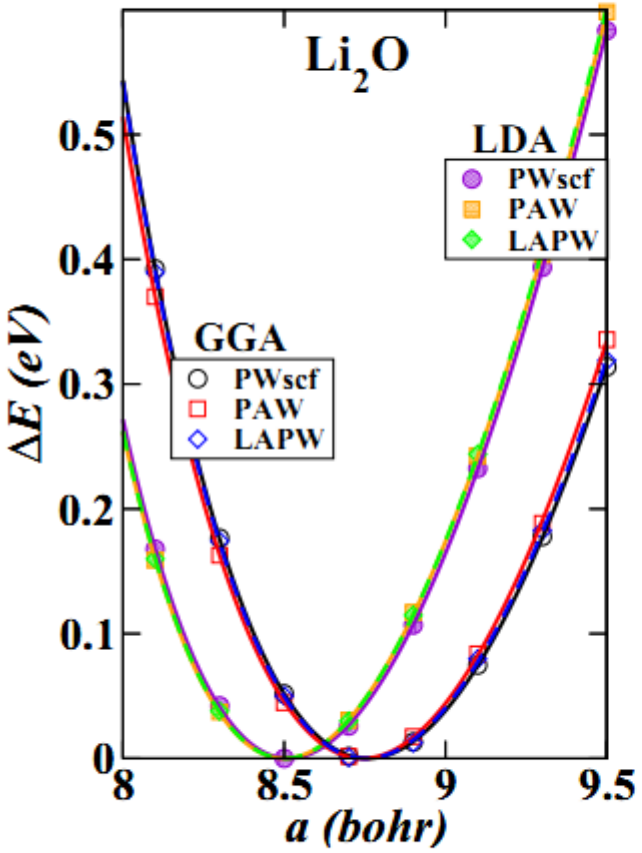

Fluorite structure

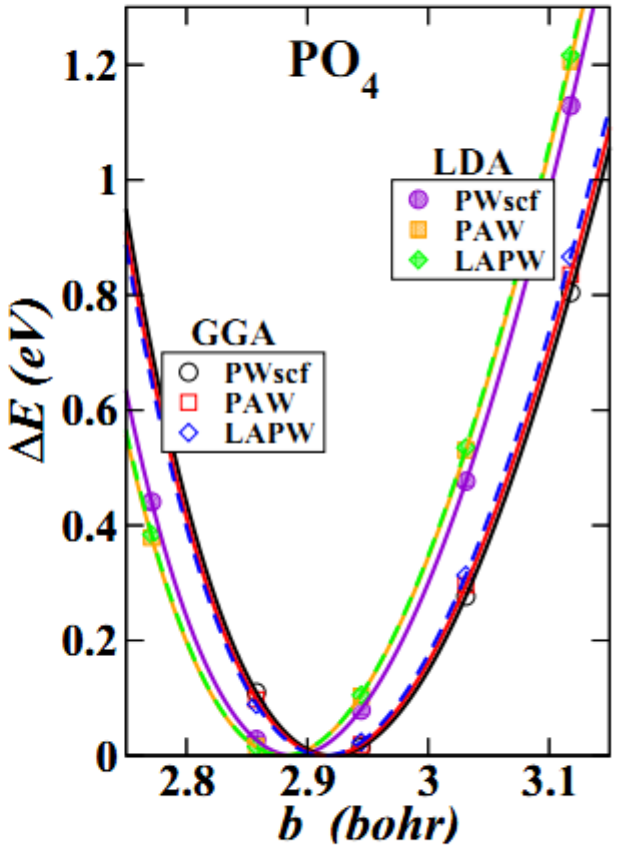

Tetrahedral molecule

Li_3PO_4 crystals

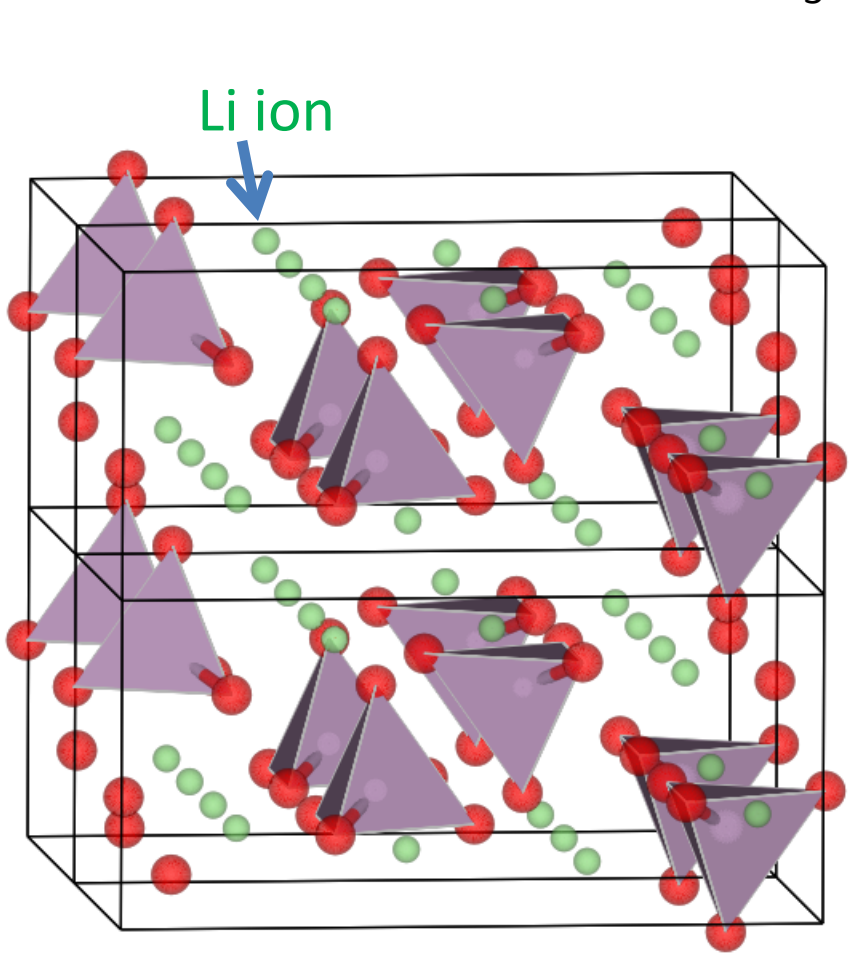

γ-Li_3PO_4 *(Pnma)*

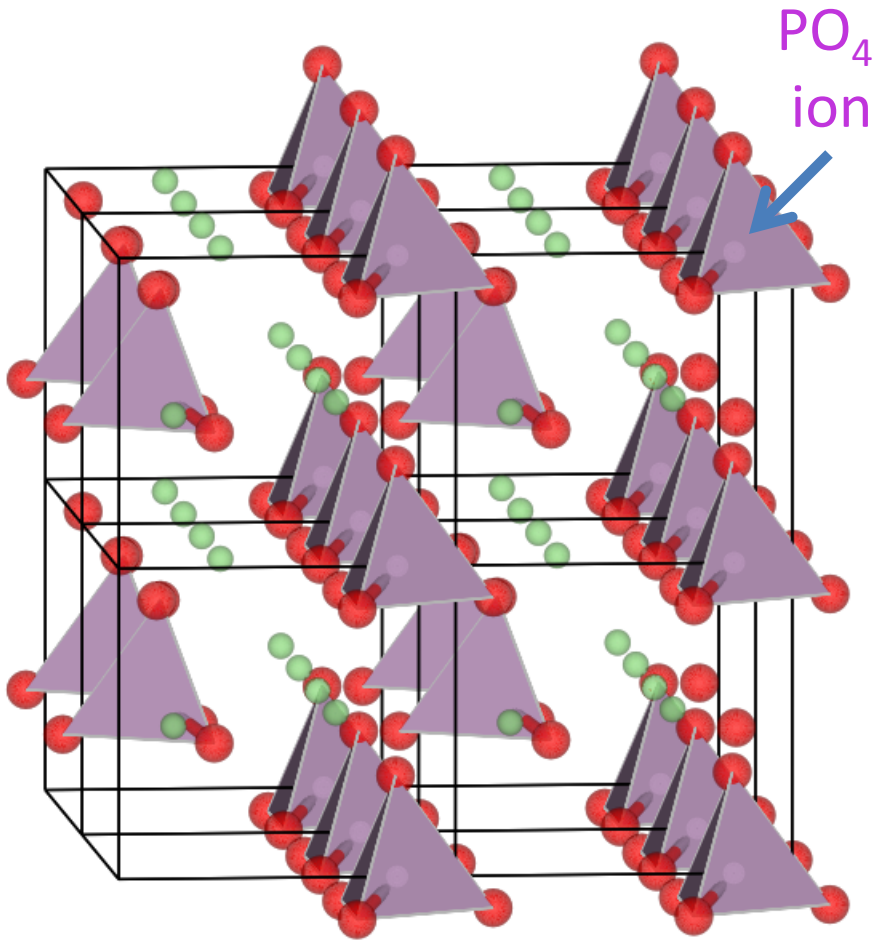

β-Li_3PO_4 *(Pnm2$_1$)*

Electron densities of states for Li_3PO_4

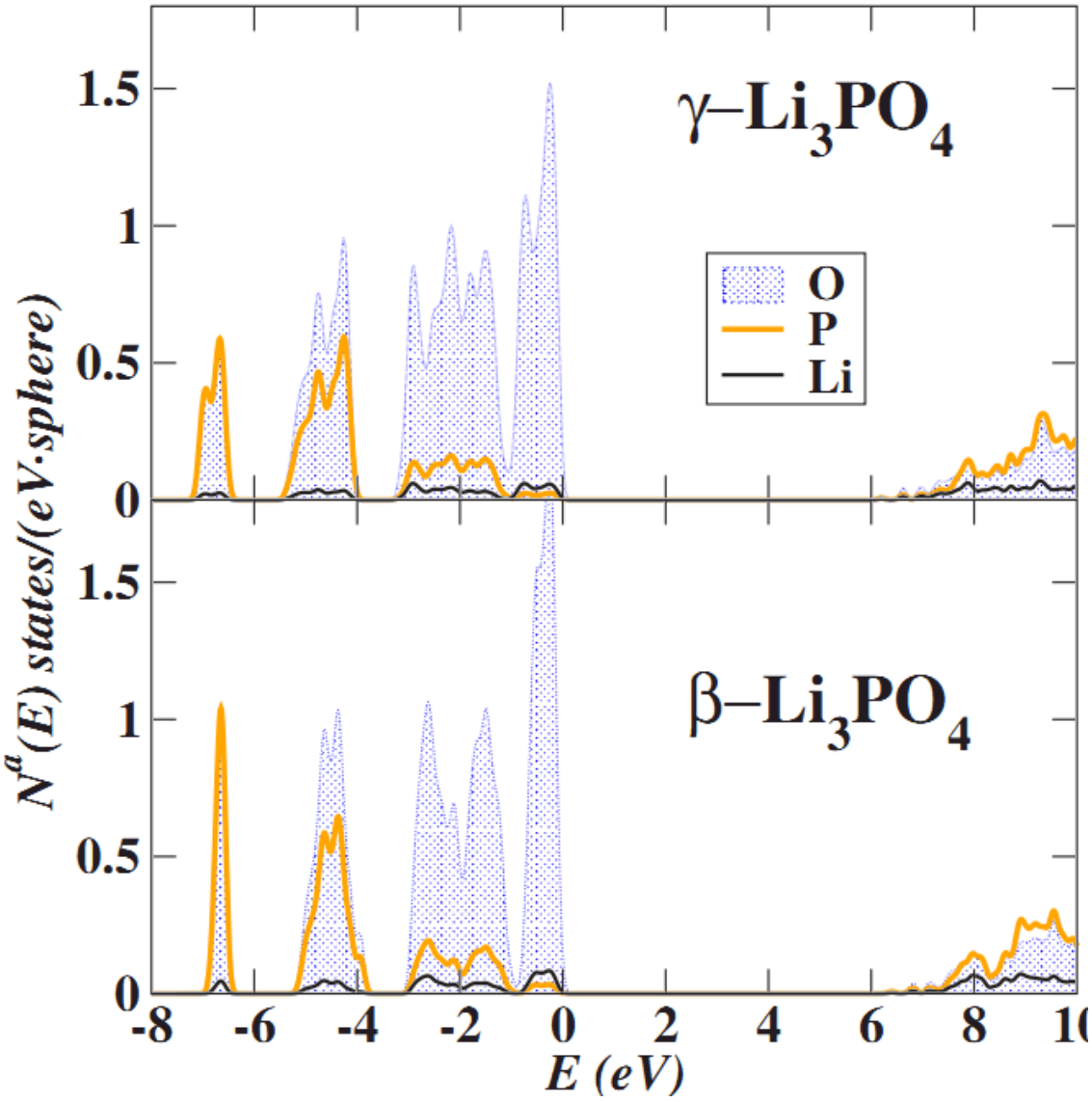

Validation of calculations

Raman spectra – Experiment & Calculation

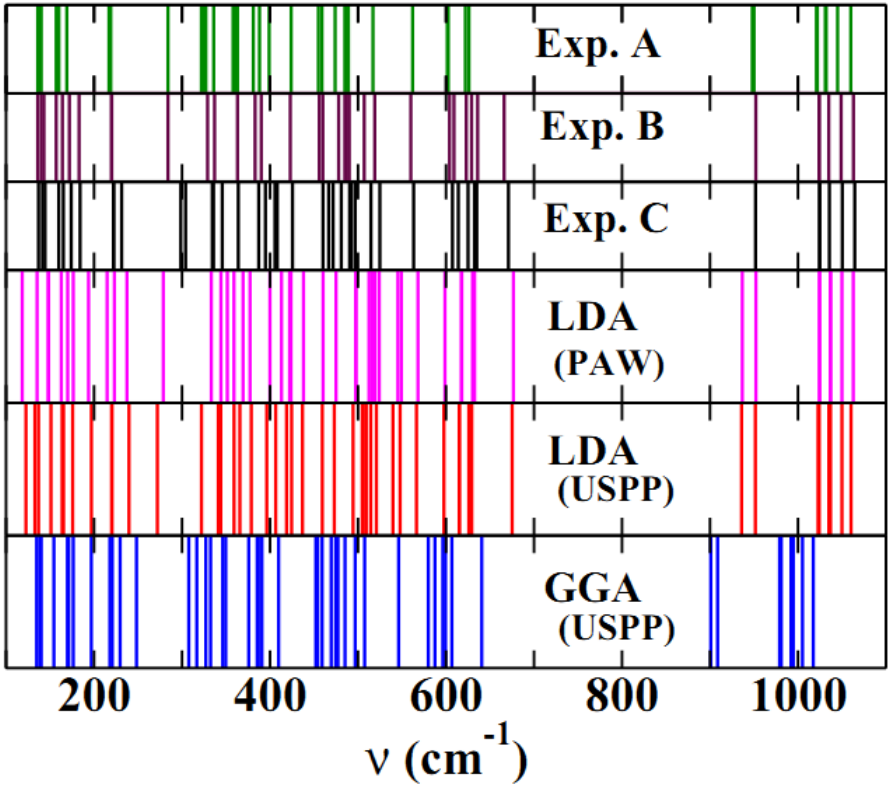

γ-Li_3PO_4

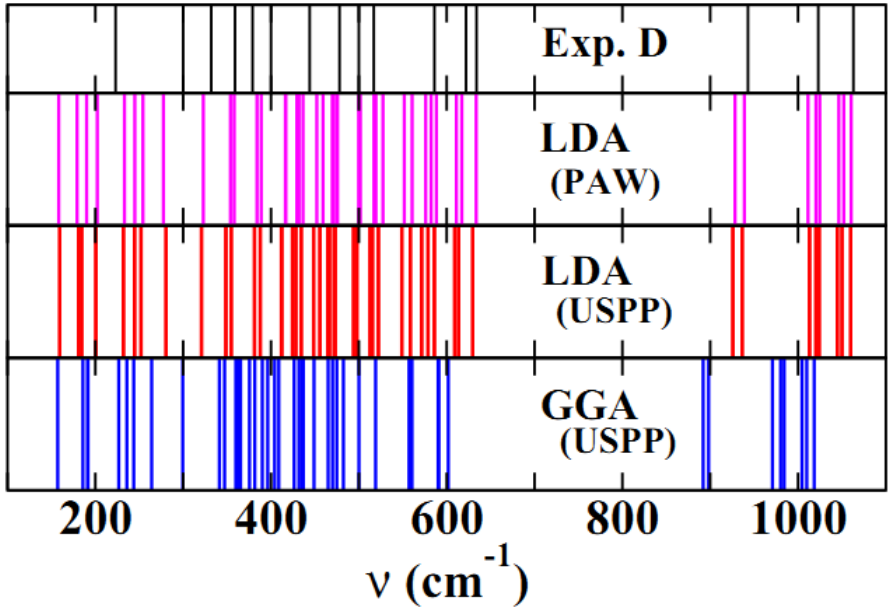

β-Li_3PO_4

A: B. N. Mavrin et al, J. Exp. Theor. Phys. **96**,53 (2003); B: F. Harbach and F. Fischer, Phys. Status Solidi B **66**, 237 (1974) – room temp. C: Ref. B at liquid nitrogen temp.; D: L. Popović et al, J. Raman Spectrosc. **34**,77 (2003).

Systematic study of LiPON materials -- $Li_xPO_yN_z$

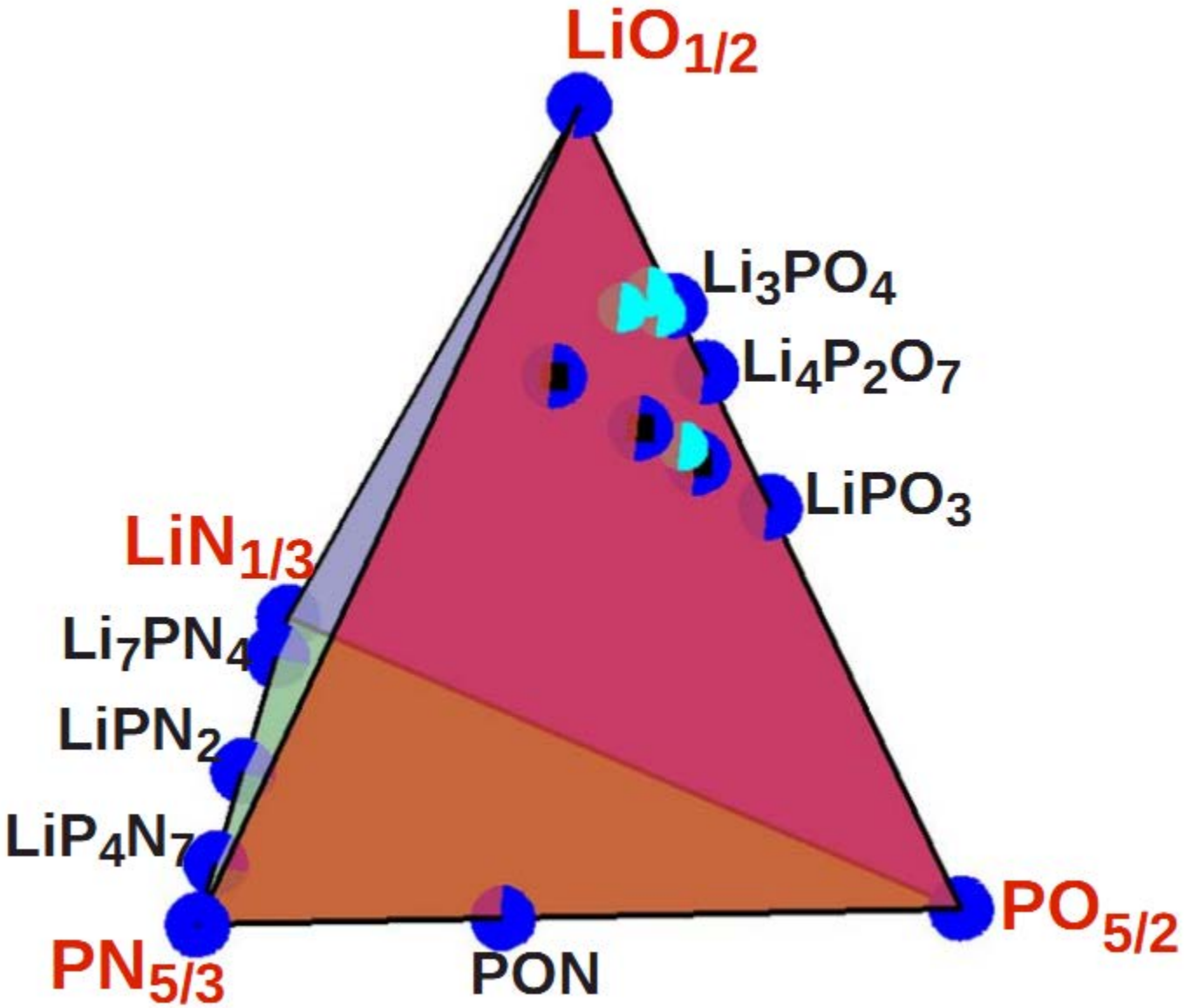

Phosphate chain materials: $LiPO_3$ plus N

$LiPO_3$ in $P2/c$ structure; 100 atom unit cell

Chain direction perpendicular to plane of diagram

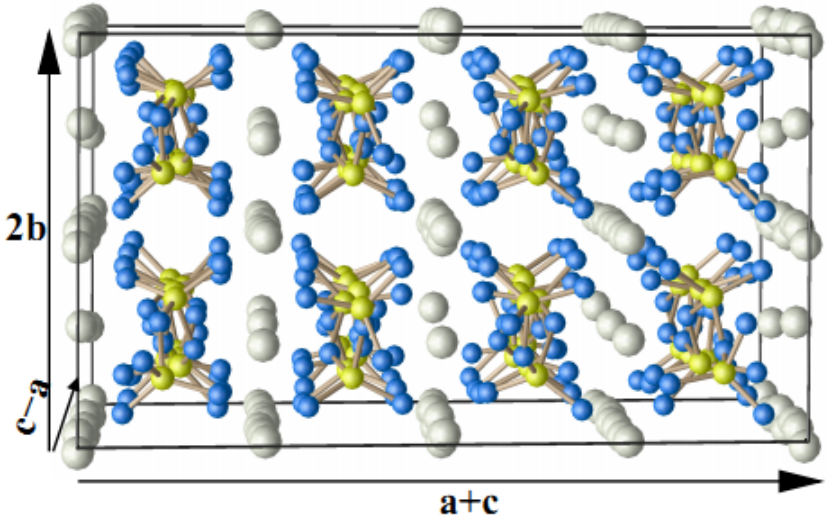

Ball colors: =Li, =P, =O.

Single chain view

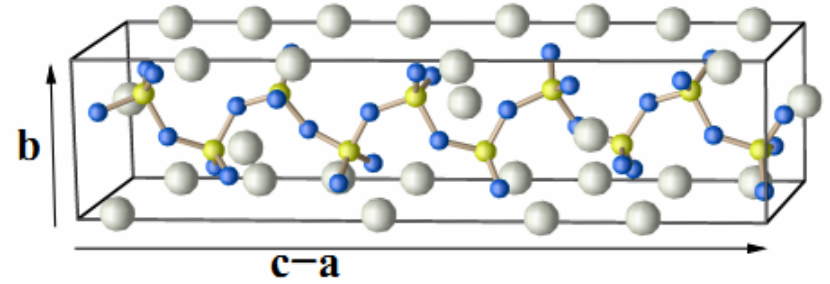

s_1-Li_2PO_2N in $Pbcm$ structure; 24 atom unit cell

Chain direction perpendicular to plane of diagram

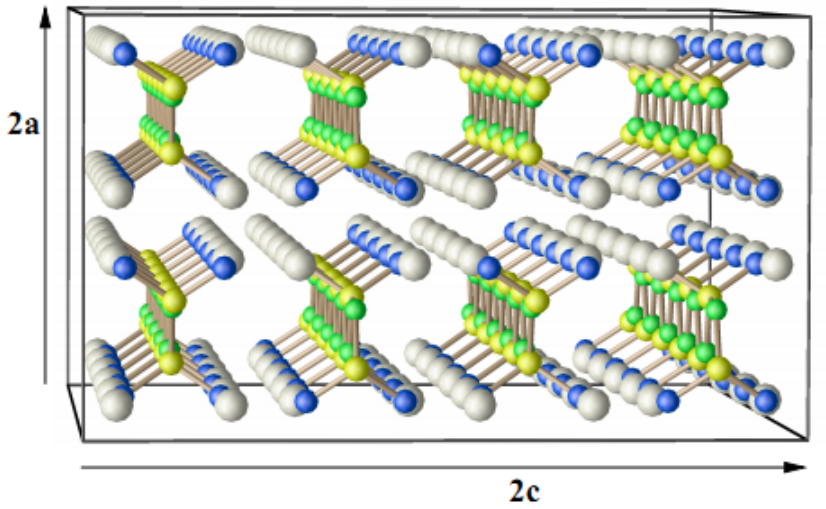

Ball colors: =Li, =P, =O, =N.

Single chain view

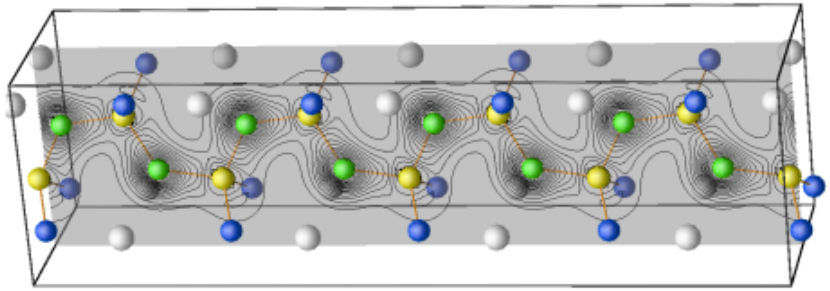

Two forms of Li_2PO_2N

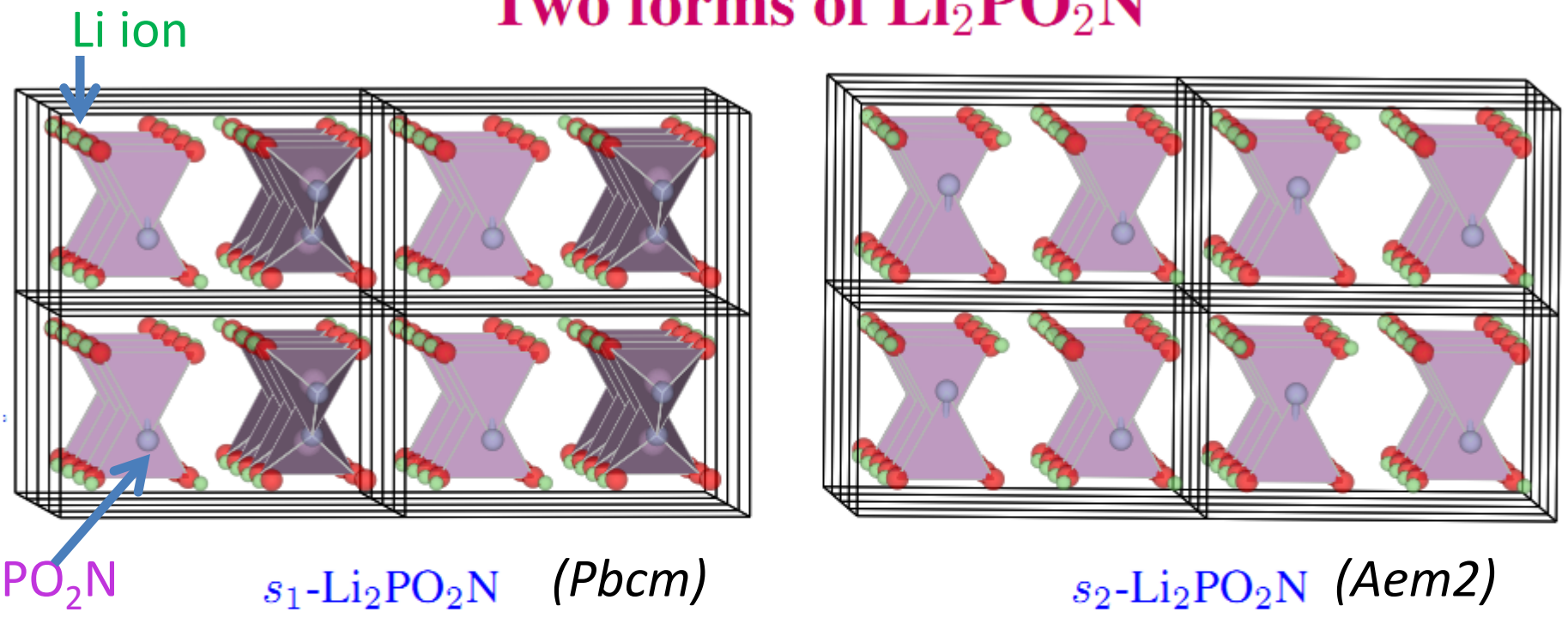

s_1-Li_2PO_2N *(Pbcm)*

s_2-Li_2PO_2N *(Aem2)*

Possible exothermic reaction pathways:

$$\tfrac{1}{5}P_2O_5 + \tfrac{1}{5}P_3N_5 + Li_2O \rightarrow Li_2PO_2N + 2.5\ \text{eV}.$$

$$Li_2O_2 + \tfrac{1}{5}P_3N_5 + \tfrac{2}{5}P \rightarrow Li_2PO_2N + 5.3\ \text{eV}.$$

$$LiNO_3 + Li + P \rightarrow Li_2PO_2N + \tfrac{1}{2}O_2 + 7.0\ \text{eV}.$$

Synthesis of Li_2PO_2N by Keerthi Senevirathne, Cynthia Day, Michael Gross, and Abdessadek Lachgar

Method: High temperature solid state synthesis based on reaction

$$Li_2O + \frac{1}{5}P_2O_5 + \frac{1}{5}P_3N_5 \rightarrow Li_2PO_2N$$

Structure from X-ray refinement: $Cmc2_1$

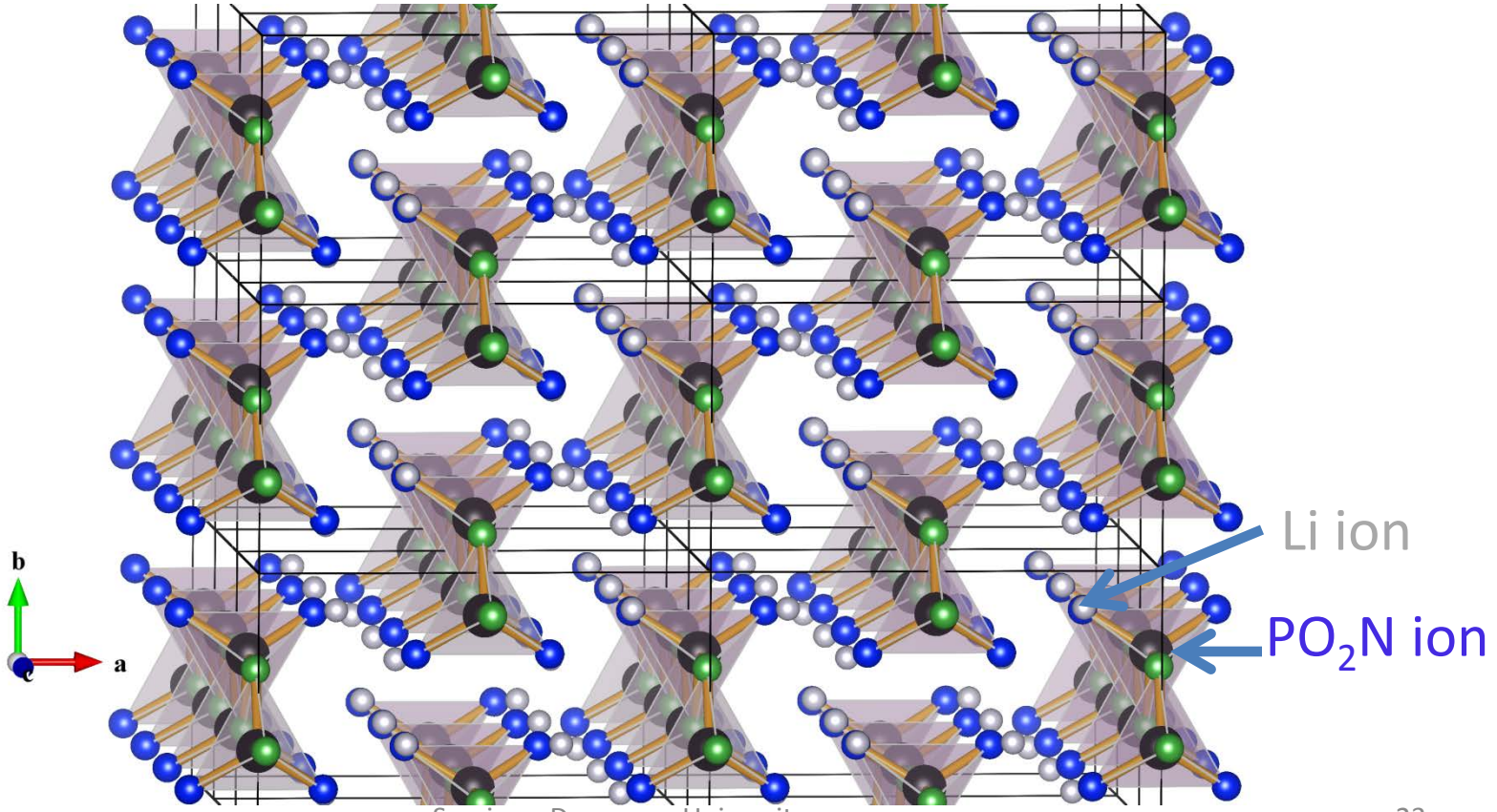

Comparison of synthesized and predicted structures of Li_2PO_2N:

Synthesized

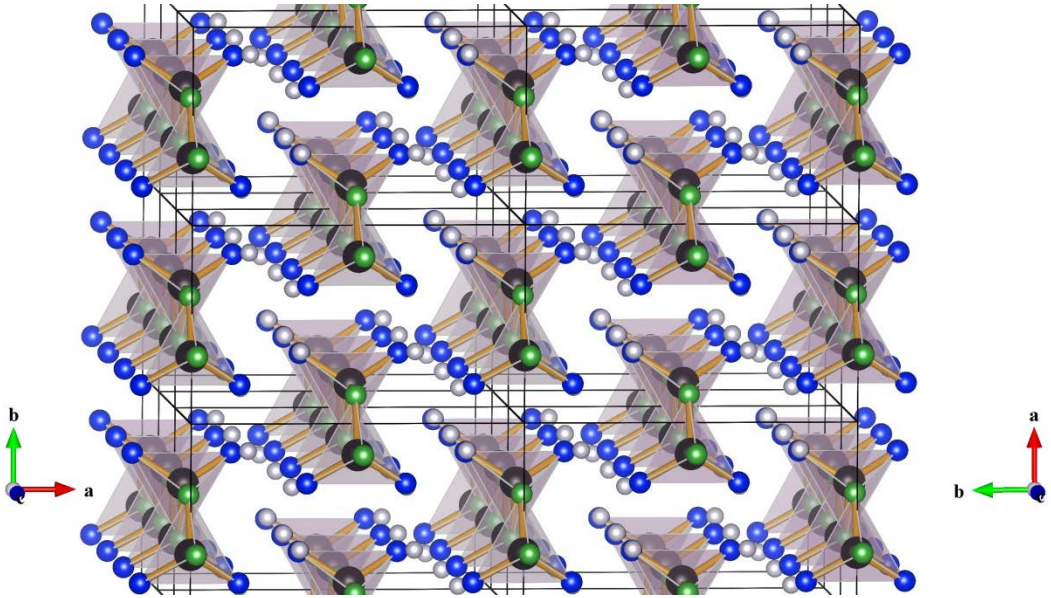

Predicted

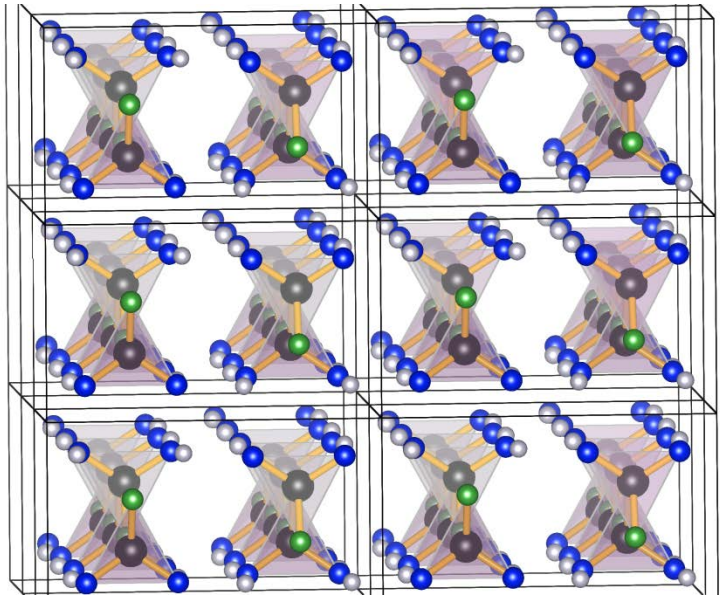

***SD*-Li_2PO_2N (*$Cmc2_1$*)**

***s_2*-Li_2PO_2N (*Aem2*)**

Calculations have now verified that the SD structure is more stable than the s_2 structure by 0.1 eV/FU.

More details of *SD*-Li_2PO_2N structure

Ball and stick model

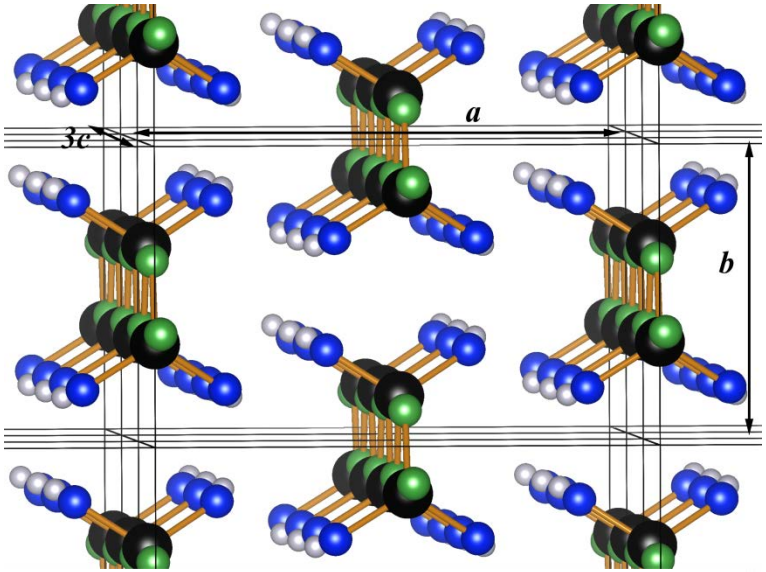

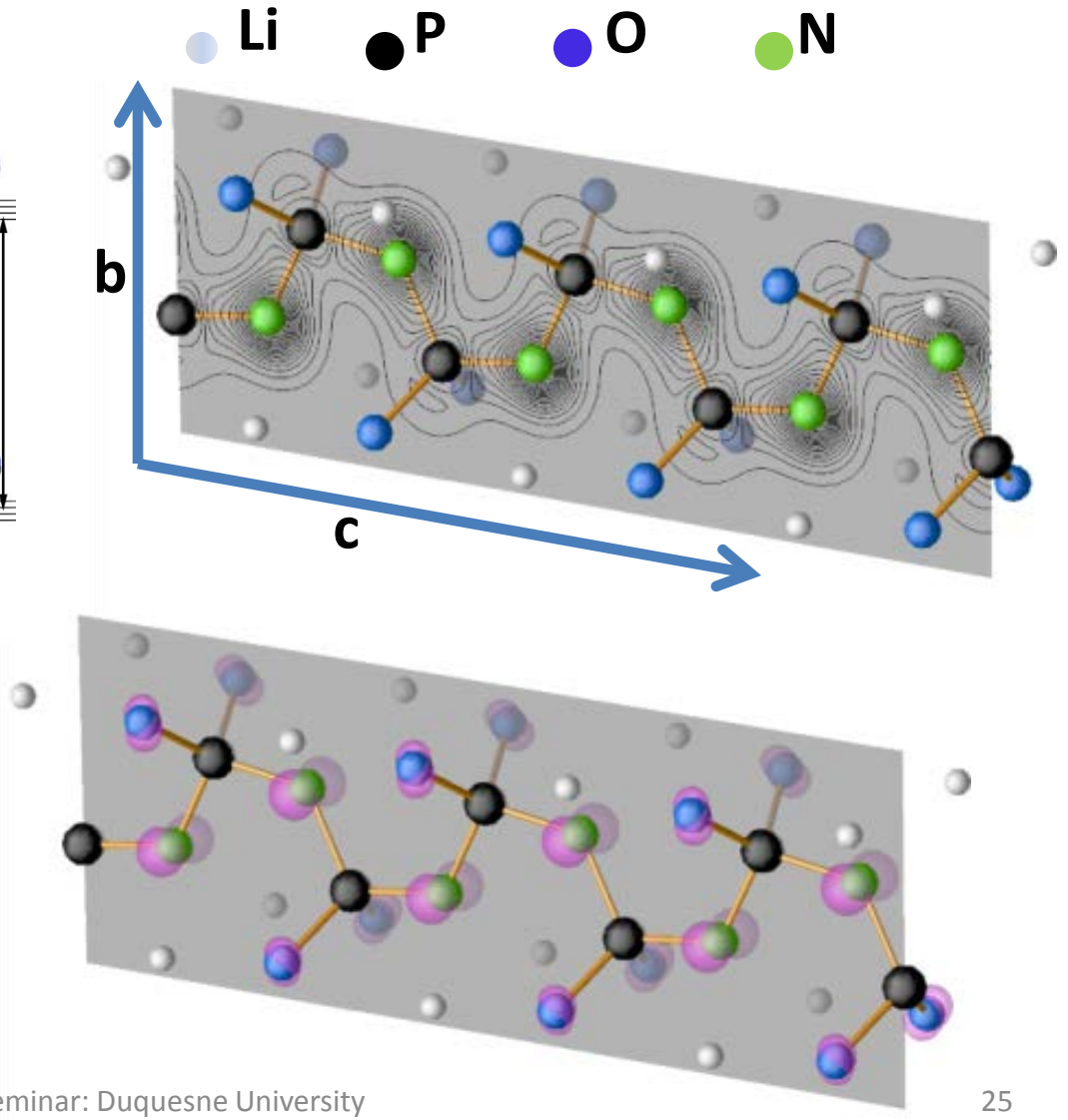

Isosurfaces (maroon) of charge density of states at top of valence band.

Electronic band structure of *SD*-Li_2PO_2N

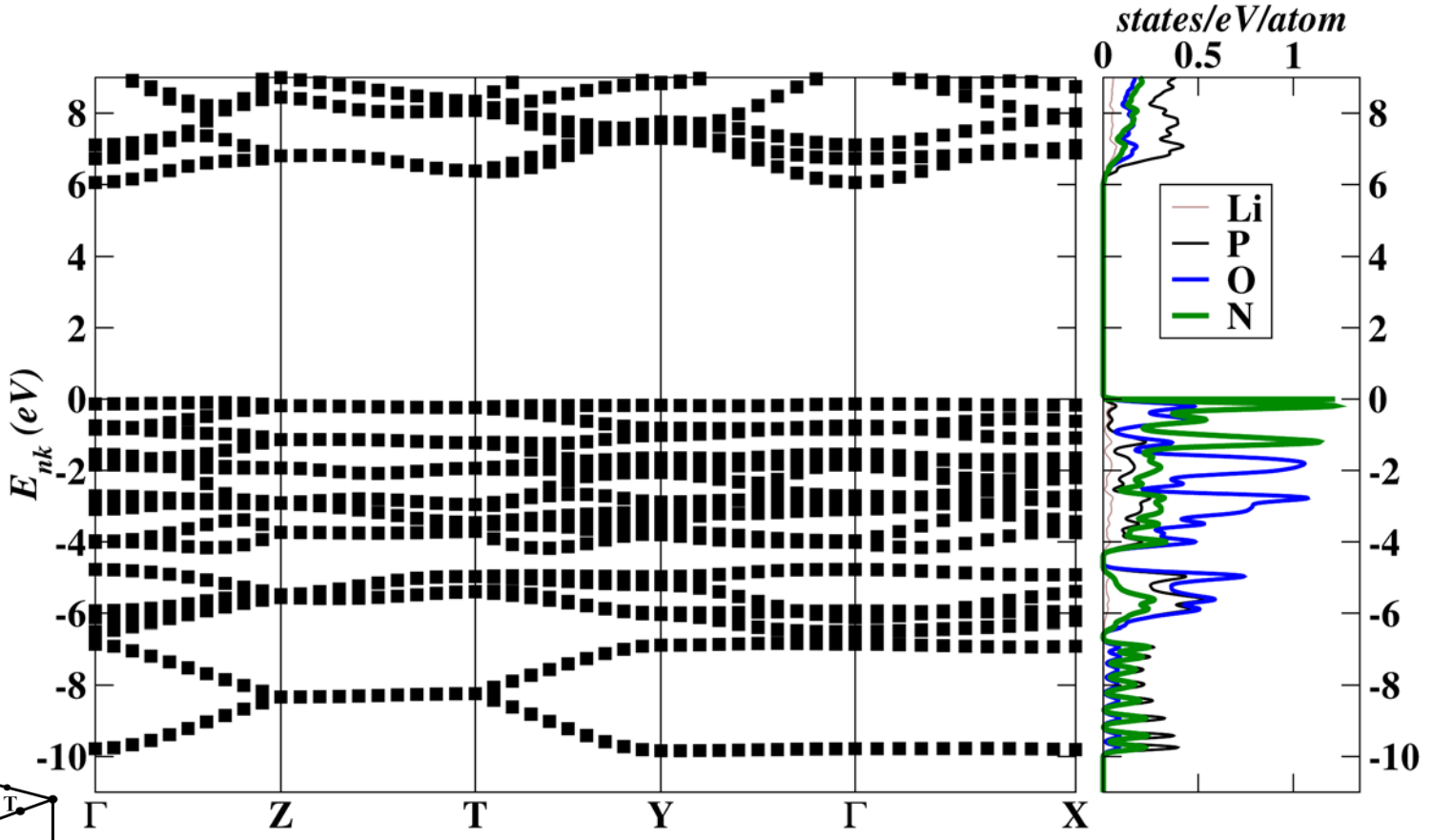

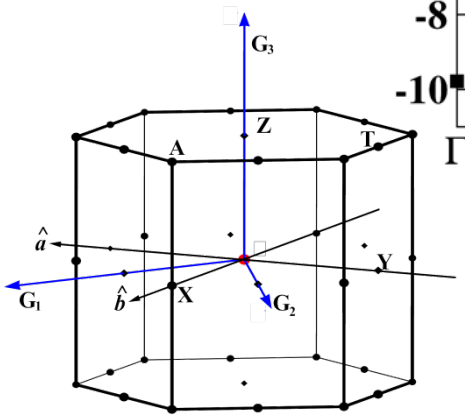

Vibrational spectrum of *SD*-Li_2PO_2N

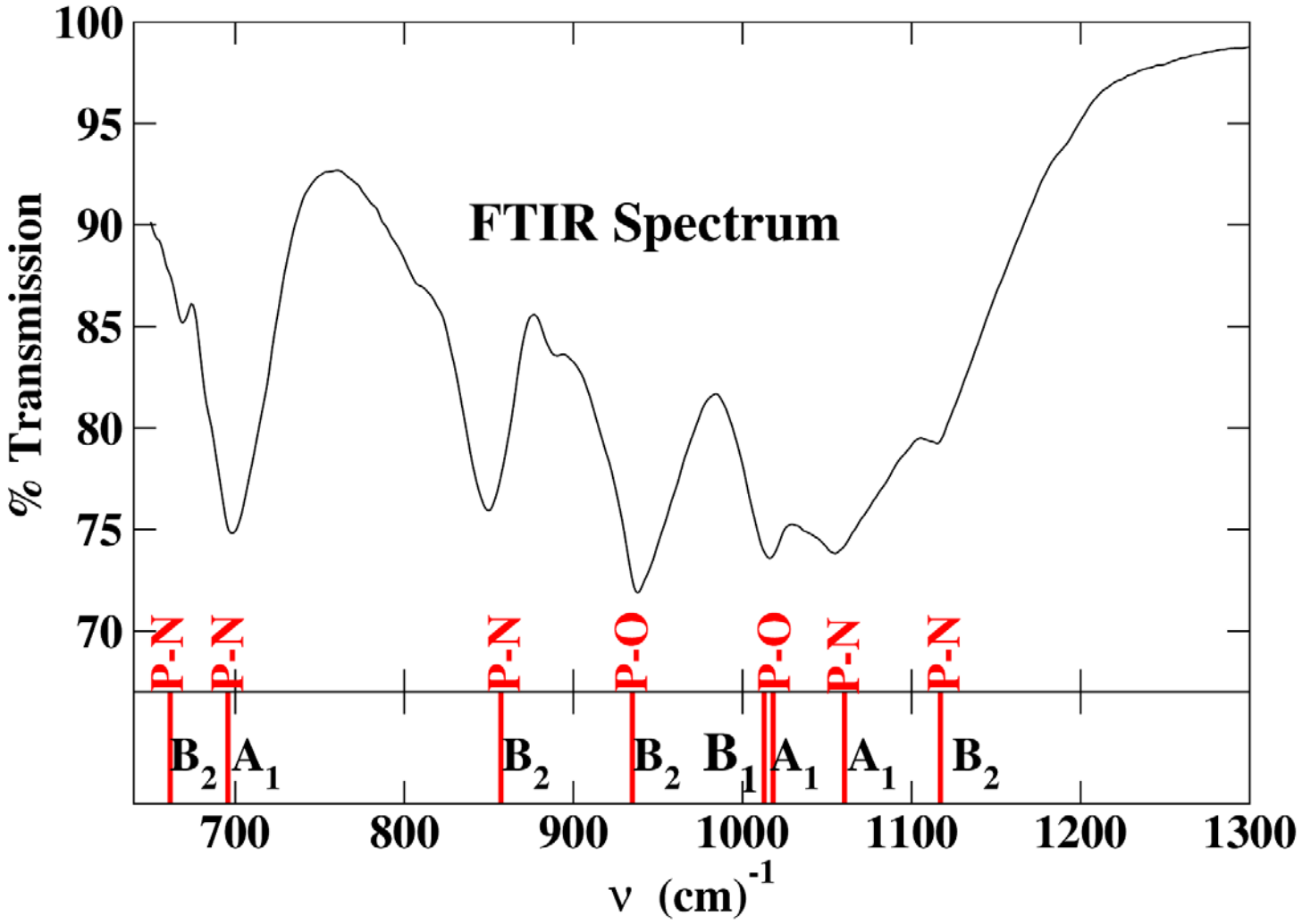

Ionic conductivity of *SD*-Li_2PO_2N

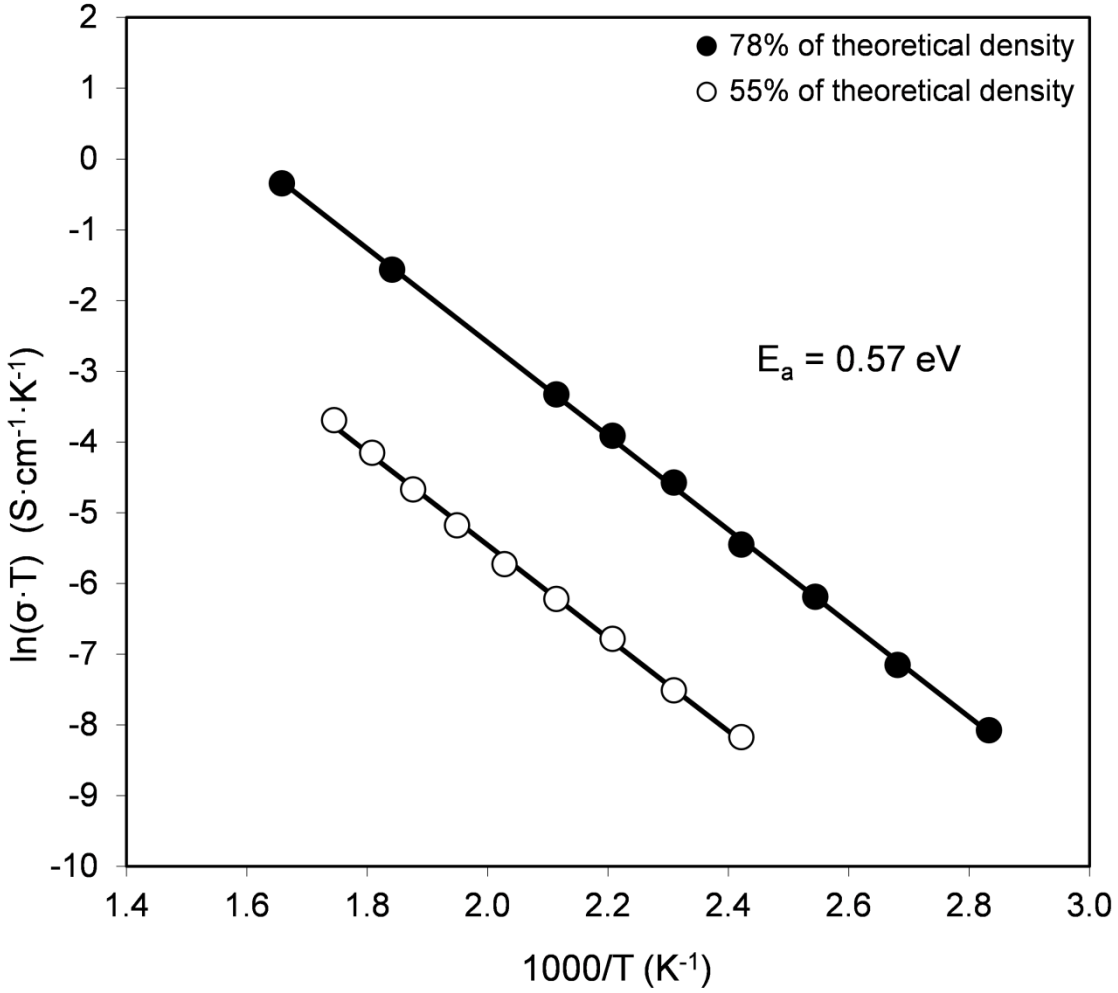

NEB analysis of E_m (vacancy mechanism)

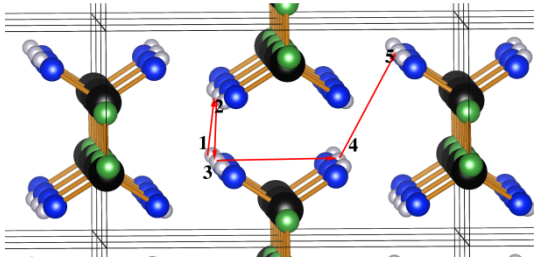

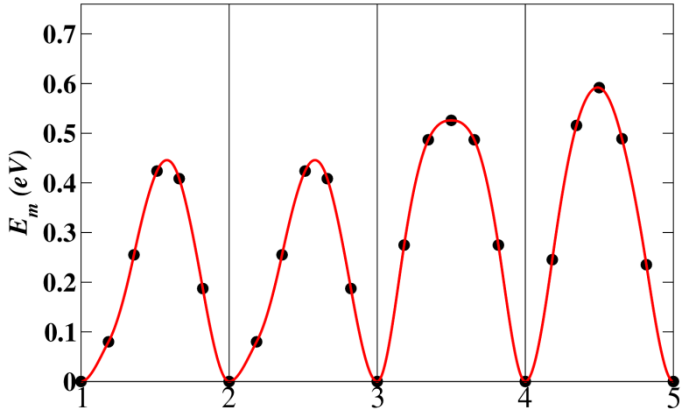

Summary of measured and calculated conductivity parameters in $Li_xPO_yN_z$ materials

Measured activation energies E_A^{exp} compared with calculated migration energies for vacancy (E_m^{cal} (vac.)) and interstitial (E_m^{cal} (int.)) mechanisms and vacancy-interstitial formation energies (E_f^{cal}). All energies are given in eV.

Material	Form	E_A^{exp}	E_m^{cal} (vac.)	E_m^{cal} (int.)	E_f^{cal}	E_A^{cal}
γ-Li_3PO_4	single crystal[a]	1.23, 1.14	0.7, 0.7	0.4, 0.3	1.7	1.3, 1.1
$Li_{2.88}PO_{3.73}N_{0.14}$	poly cryst.	0.97				
$Li_{3.3}PO_{3.9}N_{0.17}$	amorphous	0.56				
$Li_{1.35}PO_{2.99}N_{0.13}$	amorphous	0.60				
$LiPO_3$	poly cryst.	1.4	0.6, 0.7	0.7	1.2	1.1-1.2
$LiPO_3$	amorphous	0.76-1.2				
s_1-Li_2PO_2N	single crystal		0.5, 0.6		1.7	1.3-1.5
$LiPN_2$	poly cryst.	0.6	0.4		2.5	1.7
Li_7PN_4	poly cryst.	0.5				

Other electrolyte materials -- thiophosphate

LiPON and LiS_2-P_2S_5 conductivities

X. Yu, J. B. Bates, G. E. Jellison, Jr., and F. X. Hart, J. Electrochem. Soc. **144** 524-532 (1997):

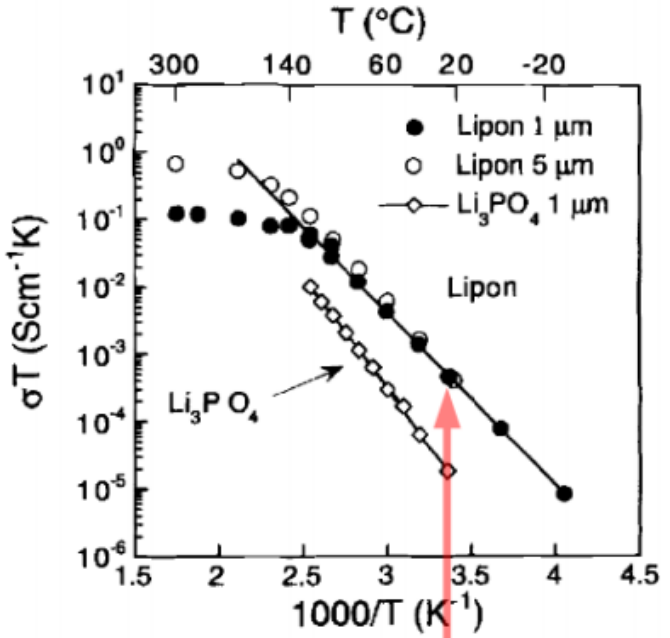

Fig. 3. Arrhenius plot of ionic conductivity of Lipon and Li_3PO_4 vs. temperature.

$\sigma = 2 \times 10^{-6}$ S/cm
$E_a = 0.5$ eV

M. Tatsumisago and A. Hayashi, J. Non-Cryst. Solids **354** 1411-1417 (2008):

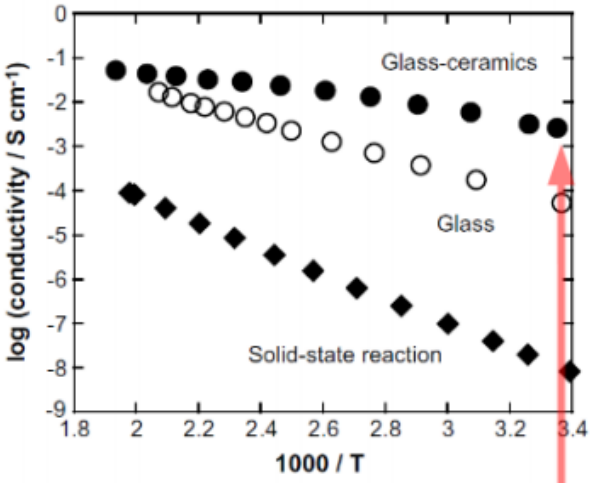

Fig. 5. Temperature dependences of the conductivities for the $70Li_2S \cdot 30P_2S_5$ glass and glass–ceramics. The conductivity data for the sample prepared by solid-state reaction are also shown.

$\sigma = 3 \times 10^{-3}$ S/cm
$E_a = 0.1$ eV

"Superionic conductor" $Li_7P_3S_{11}$

N. D. Lepley and N. A. W. Holzwarth, JES **159** A538-A547 (2012)

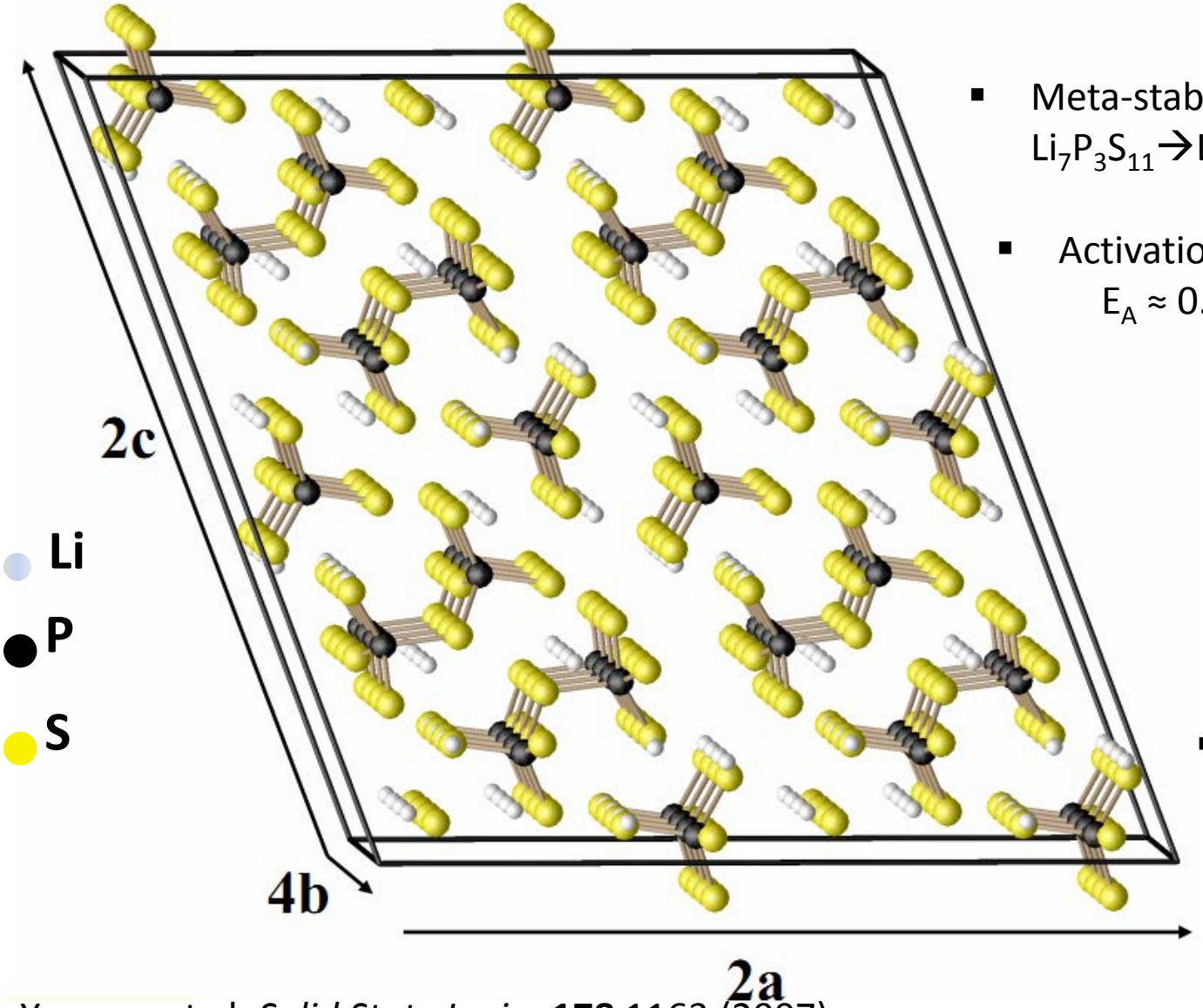

- Meta-stable to decomposition: $Li_7P_3S_{11} \rightarrow Li_3PS_4 + Li_4P_2S_6 + S$
- Activation energy estimate: $E_A \approx 0.2$ eV (Exp. 0.1 eV)

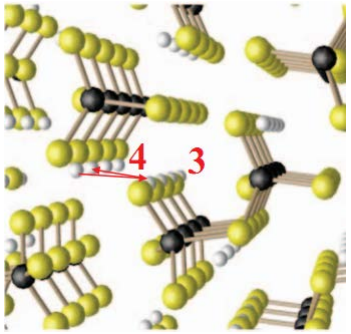

- Interstitial-vacancy pair formation energy $E_f \approx 0$

Yamane et al, *Solid State Ionics* **178** 1163 (2007)

$Li_{10}GeP_2S_{12}$ – preliminary results

Other simulation studies on this material:

Work by MIT group published in Dec. 2011

CHEMISTRY OF MATERIALS

Communication

pubs.acs.org/cm

First Principles Study of the $Li_{10}GeP_2S_{12}$ Lithium Super Ionic Conductor Material

Yifei Mo, Shyue Ping Ong, and Gerbrand Ceder*

Department of Materials Science and Engineering, Massachusetts Institute of Technology, Cambridge, Massachusetts 02139, United States

Supporting Information

KEYWORDS: *lithium ionic conductor, solid electrolyte, $Li_{10}GeP_2S_{12}$, ab initio, molecular dynamics, phase diagrams*

dx.doi.org/10.1021/cm203303y | Chem. Mater. 2012, 24, 15−17

Constituents of $Li_{10}GeP_2S_{12}$:

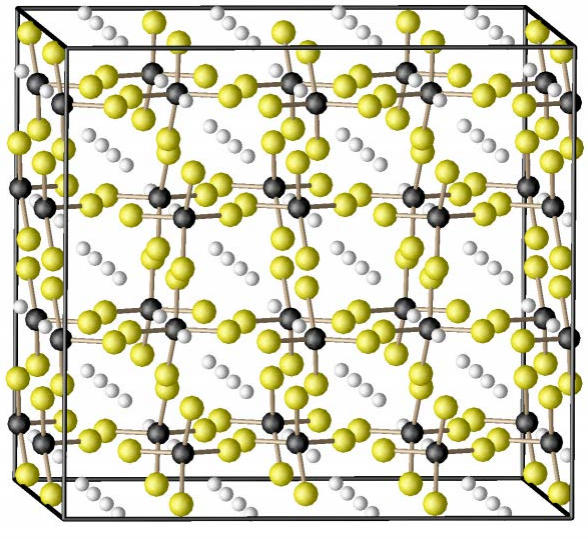

α^*- Li_3PS_4 $Pbcn$

$\Delta H = -8.12$ eV

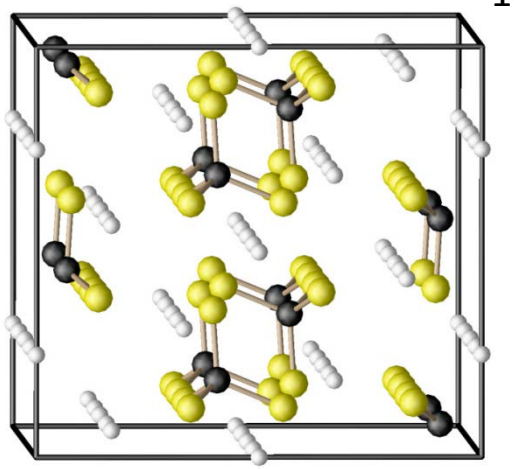

$\beta^* - Li_3PS_4$ $Pnma$

$\Delta H = -8.28$ eV

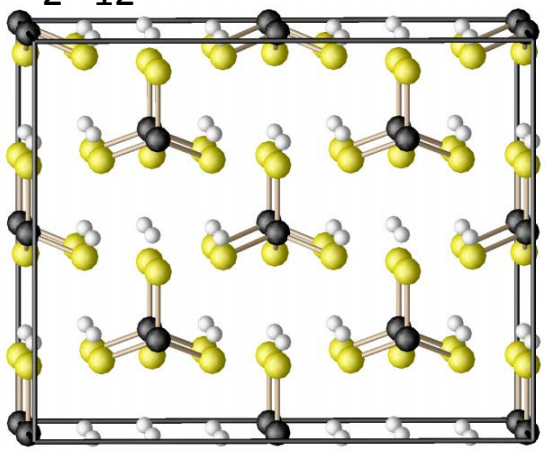

$\gamma^* - Li_3PS_4$ $Pmn2_1$

$\Delta H = -8.36$ eV

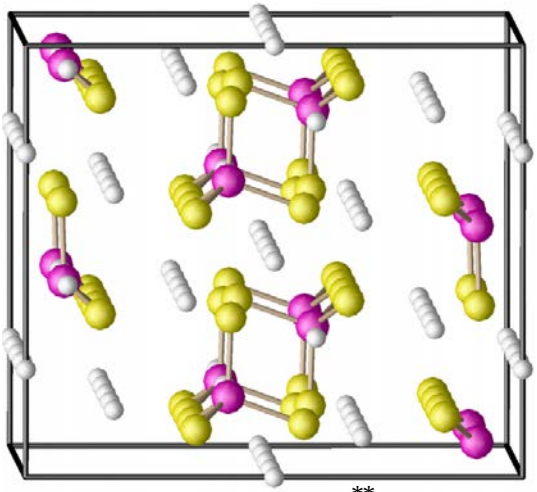

Li_4GeS_4 $Pnma^{**}$

$\Delta H = -10.19$ eV

- S
- Li
- P
- Ge

*K. Homma et al, *Solid State Ionics* **182**, 53-58 (2011)

M. Murayama et al, *Solid State Ionics* **154-155, 789-794 (2002)

$Li_{10}GeP_2S_{12}$

Space group $P4_2/nmc$ (#137)

(from experiment)

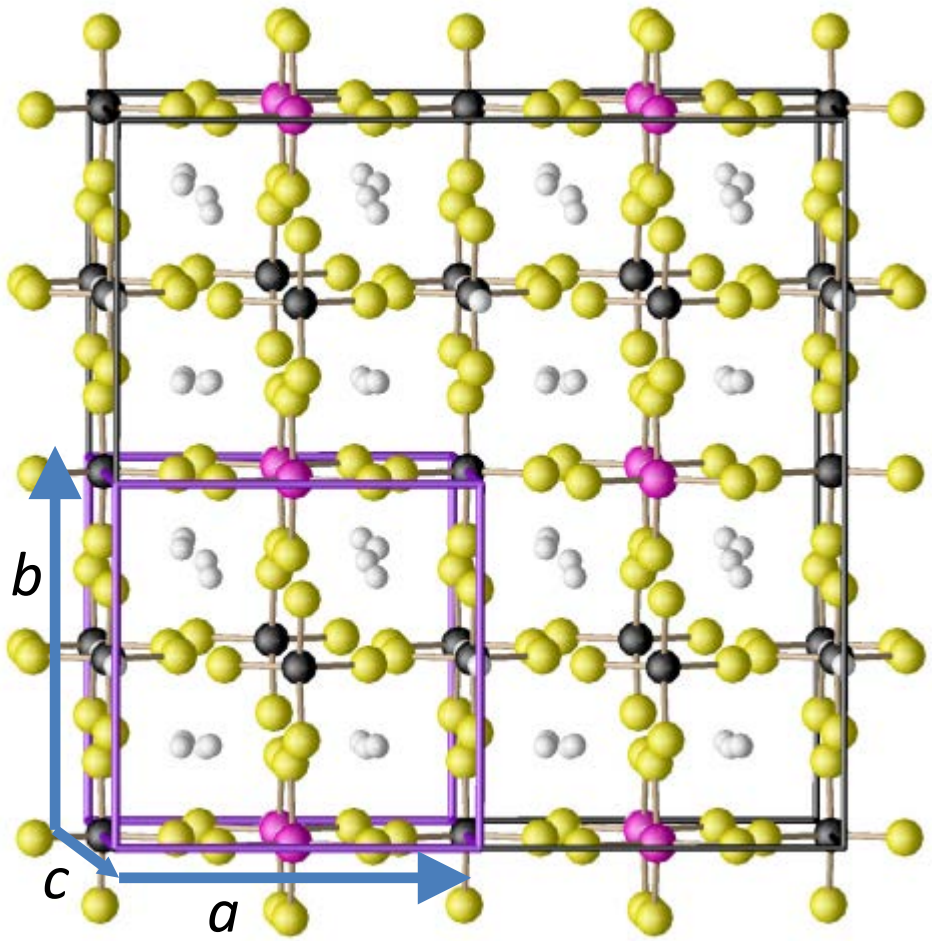

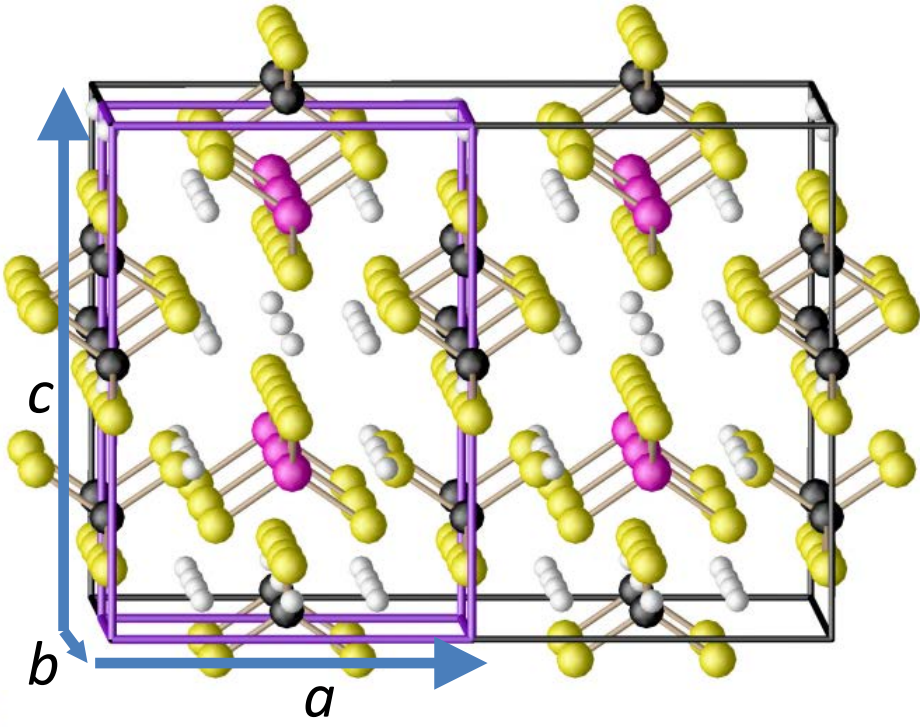

S
Li
P
Ge

Lattice parameters

	a (Å)	*c* (Å)
$Li_{10}GeP_2S_{12}$ (exp*)	8.72	12.63
$Li_{10}GeP_2S_{12}$ (Calc)	8.56	12.23
$Li_{10}SiP_2S_{12}$ (Calc)	8.55	12.16

*Kamaya et al, *Nature Materials* **10**, 682-686 (2011)

Experimentally determined symmetry (fractional occupancy):
Space group $P4_2/nmc$ (#137)

Optimized structure with full occupancy:*
Space group $P4_2mc$ (#105)

$$(x, y, z) \rightarrow (y, x, -z)$$

*Determined using FINDSYM written by Stokes, Campbell, and Hatch at Brigham Young U. – http://stokes.byu.edu/iso/

Experiment structure:
Space group $P4_2/nmc$ (#137)

Atom	g	x	y	z
Li(1) 16h	0.69	0.26	0.27	0.18
Li(2) 4d	1.00	0.00	0.50	0.94
Li(3) 8f	0.64	0.25	0.25	0.00
Ge(1) 4d	0.52	0.00	0.50	0.69
P(1) 4d	0.49	0.00	0.50	0.69
Ge(2) 2b	0.00	0.00	0.00	0.50
P(2) 2b	1.00	0.00	0.00	0.50
S(1) 8g	1.00	0.00	0.18	0.41
S(2) 8g	1.00	0.00	0.30	0.10
S(3) 8g	1.00	0.00	0.70	0.79

Calculated structure:
Space group $P4_2mc$ (#105)*

Atom	g	x	y	z
Li(1) 8f	1.00	0.23	0.23	0.29
Li(2) 2a/2b	1.00	0.00	0.50	0.94
Li(3) 8f	1.00	0.26	0.22	0.03
Ge(1) 2b	1.00	0.50	0.00	0.79
P(1) 2a	1.00	0.00	0.50	0.68
P(2) 2c	1.00	0.00	0.00	0.50
S(1) 4d/4e	1.00	0.00	0.20	0.41
S(2) 4d/4e	1.00	0.00	0.30	0.09
S(3) 4d/4e	1.00	0.00	0.70	0.78

*Wyckoff symbols for #105, coordinates in #137 convention.

Decomposition reactions predicted on the basis of calculated enthalpies of formation (at zero temperature)

	ΔH (eV)
$Li_{10}GeP_2S_{12} \rightarrow 2Li_3PS_4 + Li_4GeS_4$	0.77
$Li_{10}SiP_2S_{12} \rightarrow 2Li_3PS_4 + Li_4SiS_4$	0.74
$Li_{13}GeP_3S_{16} \rightarrow 3Li_3PS_4 + Li_4GeS_4$	0.55
$Li_{13}SiP_3S_{16} \rightarrow 3Li_3PS_4 + Li_4SiS_4$	0.62

➔Preliminary results for formation enthalpies from zero-temperature simulations predict all of the compounds to be unstable with respect to their constituents.

➔Work continuing to investigate Li ion migration energies.

Summary and conclusions

- Ideal research effort in materials includes close collaboration of both simulations and experimental measurements.
- For battery technology, there remain many opportunities for new materials development.
- Case studies carried out by our group for solid electrolyte materials including Li phosphorus oxinitrides, Li thiophosphates, and very preliminary results for materials containing thiogerminates.